CHALMERS
UNIVERSITY OF TECHNOLOGY

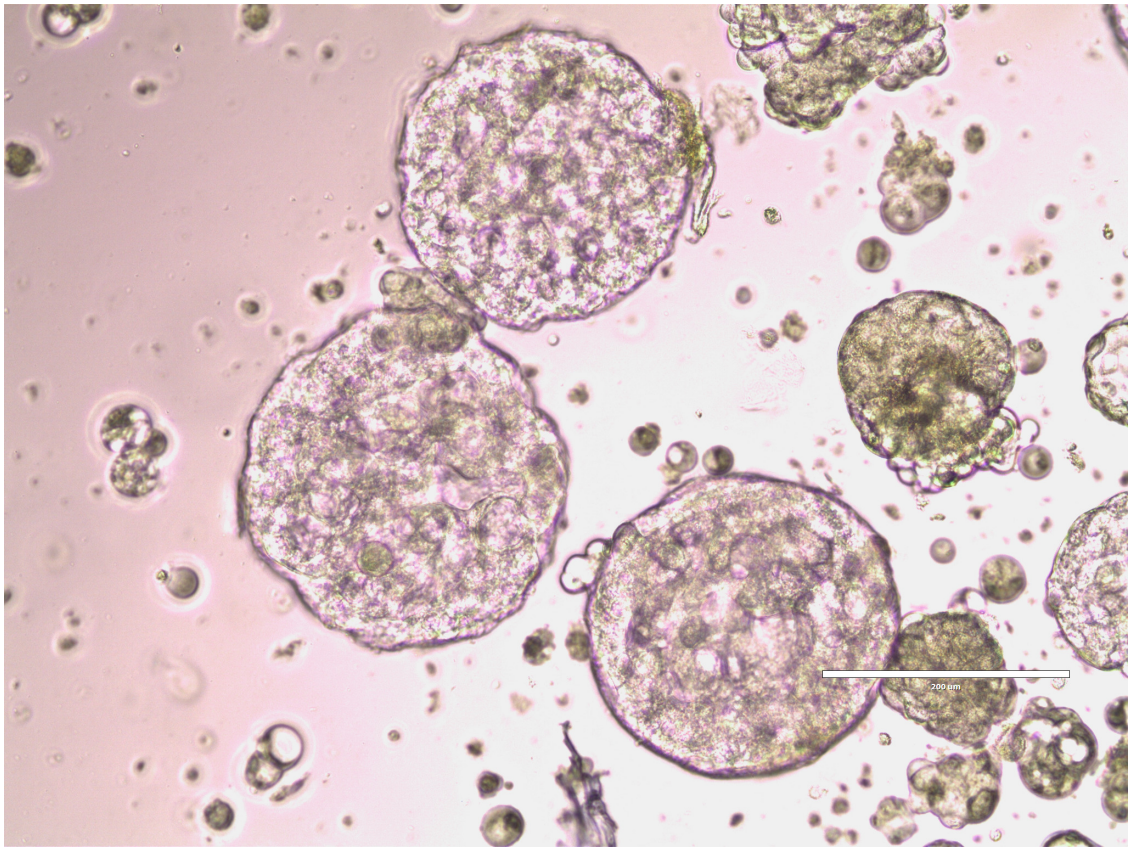

Enhanced CA15-3 Production Using Microcarrier-Based ZR75-1 Cultures

Development and Optimization of a Suspension-Like Bioprocess for ZR75-1 Cells for Efficient CA15-3 Tumor Marker Production

Master's thesis in Biotechnology

STINA BJÖRNELF

DEPARTMENT OF LIFE SCIENCES

CHALMERS UNIVERSITY OF TECHNOLOGY
Gothenburg, Sweden 2025
www.chalmers.se

Master's thesis 2025

Enhanced CA15-3 Production Using Microcarrier-Based ZR75-1 Cultures

Development and Optimization of a Suspension-Like Bioprocess for Efficient CA15-3 Tumor Marker Production

STINA BJÖRNELF

CHALMERS
UNIVERSITY OF TECHNOLOGY

Department of Life Sciences
Chalmers University of Technology
Gothenburg, Sweden 2025

Enhanced CA15-3 Production Using Microcarrier-Based ZR75-1 Cultures
Development and Optimization of a Suspension-Like Bioprocess for Efficient CA15-3 Tumor Marker Production
STINA BJÖRNELF

Supervisor: Lina Lövgren, M. Sc Supervisor Bioreagent Process Improvement
Fujirebio Diagnostics AB
lina.lovgren@fdab.com

Examiner: Anna Karlsson-Bengtsson, Professor
Division of Chemical Biology
Chalmers University of Technology
anna.karlsson-bengtsson@chalmers.se

Master's Thesis 2025
Department of Life Science
Chalmers University of Technology
SE-412 96 Gothenburg
Telephone +46 31 772 1000

Cover: Microscopic image of ZR75-1 cells on CultiSpher G microcarriers.

Typeset in LaTeX
Printed by Chalmers Reproservice
Gothenburg, Sweden 2025

Enhanced CA15-3 Production Using Microcarrier-Based ZR75-1 Cultures
Development and Optimization of a Suspension-Like Bioprocess for Efficient CA15-3 Tumor Marker Production
STINA BJÖRNELF
Department of Life Sciences
Chalmers University of Technology

Abstract

Fujirebio Diagnostics AB (FDAB) produce tumour markers for clinical diagnostics, including CA15-3, which is used to monitor breast cancer. Currently, CA15-3 is produced using ZR75-1 cells cultured in roller flasks, a manual, time-consuming process with limited scalability. To improve this, there is growing interest in transitioning to bioreactor-based systems using microcarriers, which offer higher surface area-to-volume ratios suitable for adherent cell growth. This thesis explores whether microcarrier-based cultivation can improve CA15-3 production and serve as a scalable alternative to the roller bottle process. ZR75-1 cells were cultured on various microcarriers (CultiSpher G, Corning Enhanced Attachment, BioNOC II, and Fibra-Cel) in spinner flasks, and antigen levels (CA15-3, CA125, and CEA) were monitored. Attachment efficiency, cell density, and viability were also assessed. CultiSpher G showed the best performance and was used in bioreactor trials with perfusion. Peak productivity in spinner cultures reached 23 kU/L/day, about 167% higher than estimated roller flask levels. In contrast, bioreactor productivity reached 3.7 kU/L/day but was limited by premature perfusion and cell density loss. These findings demonstrate that microcarrier cultures, particularly with CultiSpher G, can significantly enhance CA15-3 production and have strong potential for scale-up. Further optimization of attachment, perfusion timing, and bioreactor conditions is needed. Transitioning to such systems could reduce manual handling at FDAB and improve process efficiency for future antigen production.

Keywords: CA15-3 antigen, Adherent cell culture, Microcarrier technology, ZR75-1 breast cancer cells, Perfusion bioreactor, Spinner flask cultivation, Cell attachment kinetics, Bioprocess optimization.

Acknowledgements

I would like to express my gratitude to Fujirebio Diagnostics AB for the opportunity to conduct my Master's thesis project within their organization. It has been a valuable and rewarding experience to be part of a professional environment where I was welcomed and supported throughout my work.
A special thanks to my supervisor Lina Lövgren for her continuous guidance, encouragement, and feedback. Your support has been invaluable. From planning experiments to interpreting results and reviewing my writing, always taking the time to answer my questions and share your expertise.
I also want to thank all the employees at Fujirebio whom I had the pleasure of working with. Thank you for making me feel like part of the team and for sharing your knowledge, time, and humor. Your helpfulness and engagement made my experience both educational and enjoyable.
Lastly, I would like to thank Anna Karlsson-Bengtsson for taking on the role as my examiner and for helping me during the thesis process.
To everyone who contributed in one way or another – thank you.

Stina Björnelf, Gothenburg, June 2025

List of Acronyms

Below is the list of acronyms that have been used throughout this thesis listed in alphabetical order:

ATF	Alternating Tangential Flow
CA15-3	Cancer Antigen 15-3
CA125	Cancer Antigen 125
CEA	Carcinoembryonic Antigen
CSPR	Cell-Specific Perfusion Rate
DEAE	Diethylaminoethyl
DMEM	Dulbecco's Modified Eagle Medium
DO	Dissolved Oxygen EIA
Enzymatic Immunoassay	
ELISA	Enzyme-Linked Immunosorbent Assay
ECM	Extracellular Matrix
FBS	Fetal Bovine Serum
hBM-MSC	Human Bone Marrow-derived Mesenchymal Stem Cell
MCB	Master Cell Bank PBS
Phosphate-Buffered Saline	
rpm	Revolutions Per Minute
SD	Standard Deviation
STBR	Stir Tank Bioreactor
WCB	Working Cell Bank
ZR75-1	Human breast cancer cell line used for CA15-3 production

Contents

List of Figures

List of Tables

1

Introduction

As the need for high-quality tumour markers grows, so does the importance of developing more effective production systems. Tumour markers play a vital role in the early detection, monitoring, and management of cancer, and among them, Cancer Antigen 15-3 (CA15-3) is widely used in breast cancer diagnostics. To meet the increasing demand, diagnostic manufacturers must transition from labour-intensive methods to more scalable and robust culture technologies.

Fujirebio Diagnostics AB (FDAB), located in Gothenburg, Sweden, is part of the international Fujirebio Group, and specializes in the development and production of tumour markers used in *in vitro* diagnostics. FDAB has a long-standing tradition of producing monoclonal antibodies (MAbs) and tumour-associated antigens. One such product, Cancer Antigen 15-3 (CA15-3), is essential for breast cancer diagnostics and remains in high demand. Currently, CA15-3 is produced by cultivating the human breast cancer cell line ZR75-1 in cell culture roller flasks. While effective, this method is labor-intensive, physically demanding, and insufficiently scalable to meet increasing production needs.

To overcome these limitations, FDAB intends to transition from roller flask-based systems to bioreactor cultivation. Since ZR75-1 is an adherent cell line that requires a surface for attachment, scaling up necessitates an alternative growth matrix. Microcarriers, small spherical beads providing a large surface area, enable adherent cells to grow in suspension-like environments. Introduced in 1967 by van Wezel for the cultivation of human fibroblast-like cells, microcarrier technology offers scalability while maintaining process control and reducing manual labour [1, 2]. Although microcarriers have been widely used in vaccine and biopharmaceutical production [3], their application in using ZR75-1 cells for CA15-3 antigen production presents unique challenges.

This thesis aims to investigate the feasibility of microcarrier-based cultivation of ZR75-1 cells in spinner flasks and scale-up to a bench-top bioreactor. The goal is to evaluate different microcarrier types, optimize seeding and attachment conditions, and assess the potential for perfusion cultivation to enable continuous production of CA15-3. By moving away from roller flasks and toward a controlled bioreactor environment, FDAB seeks to develop a more robust and scalable platform for antigen production, ultimately improving efficiency and meeting future diagnostic needs.

1.1 Purpose

The purpose of this master's thesis was to evaluate and develop a microcarrier-based cultivation method for the adherent ZR75-1 cell line, used in the production of the breast cancer antigen CA15-3 at FDAB. The work included comparison of four different microcarriers in spinner flask cultures, ro establish a consistent method for cell counting, and analysing growth and antigen production over time. In addition, key bioreactor cultivation parameters such as stirring speed, inoculation method, and perfusion settings were tested in small-scale runs to explore their impact on cell growth and CA15-3 productivity. The aim was to provide insights and a foundation for future optimization and scale-up at FDAB.

1.2 Objectives

This project aims to:

- Compare four microcarriers for cultivation of ZR75-1 cells in spinner flask cultures.
- Establish a reliable method for counting ZR75-1 cells in microcarrier-based systems.
- Analyze cell growth, viability, and productivity over time using CA15-3, CA125, and CEA as output markers.
- Test a microcarrier-based cultivation setup in a perfusion-operated bench-top bioreactor.
- Identify key parameters affecting bioreactor performance, such as inoculation conditions, perfusion rate, and stirring speed.
- Assess whether microcarrier culture supports continued antigen production in both spinner and bioreactor systems.

1.3 Limitations and challenges

This project is limited in scope to evaluating the feasibility of using microcarriers for culturing the adherent ZR75-1 cell line to produce the tumour marker CA15-3. While the study provides insights into microcarrier-based cultivation, several limitations and challenges remain.

Only a limited set of four commercially available microcarriers were evaluated during this project. Of these, only CultiSpher® G was tested in bioreactor experiments due to cost constraints and long shipping times. As such, conclusions of microcarrier performance in the bioreactor are limited to this type of carrier. This does not reflect the full potential of other available carriers.

The cell culture medium used in all experiments remained consistent with the standard production protocol currently in use at FDAB. No modifications were made to optimize medium composition, supplementation, or to evaluate serum-free alternatives.

At FDAB, no validated method exists for accurately quantifying ZR75-1 cells, especially when grown on microcarriers. The current production process does not require routine cell density measurements, but such quantification is essential for seeding and process optimization in this project. Both manual and automated cell counting methods were evaluated and adapted as part of this work, but remain a source of variability.

Continuous stirring was applied during the attachment phase in all spinner and bioreactor cultures. The potential benefits of intermittent stirring, shown in other studies to improve attachment for certain cell types, were not explored here due to time constraints and protocol standardization.

Due to time limitations, some key parameters were not exhaustively optimized. This includes optimal microcarrier concentration, optimal cell seeding density, and attachment time before full medium addition. While general guidelines were followed, fine-tuning these variables could further improve culture performance and antigen yield.

2

Theory

2.1 Antigens and Tumour Markers

Antigens are molecules recognized by the immune system, typically through interaction with antibodies or T cell receptors. They trigger the production of antibodies by B cells [4]. Antigens can originate from a broad range of biomolecules, including proteins, carbohydrates, lipids, and nucleic acids [5]. The term "antigen" derives from this function, meaning "antibody generator."

The specific part of an antigen that is recognized by the immune system is called an epitope. Epitopes are usually short peptide sequences or distinct carbohydrate structures exposed on the surface of the antigen [5]. They can be linear (continuous amino acid sequences) or conformational (discontinuous sequences brought together by protein folding) [6]. A single antigen can contain multiple epitopes, which allows it to be recognized by several different antibodies [4].

Tumour markers are substances produced either by cancer cells or by the body in response to cancer. Thousands of tumour markers have been identified, including antigens, cytokines, metabolites, and hormones. Classical tumour markers are typically protein-based antigens, such as carcinoembryonic antigen (CEA), carbohydrate antigen 19-9 (CA19-9), and carbohydrate antigen 125 (CA125) [7]. While all cells release proteins into circulation, tumour cells often do so at significantly higher levels, leading to elevated concentrations of tumour markers in blood or other body fluids [8].

These markers are commonly detected in blood, urine, or tissue samples and are used in clinical oncology to support diagnosis, monitor treatment efficacy, and detect recurrence. However, due to limited sensitivity and specificity, they are generally not suitable for screening asymptomatic individuals [9].

Tumour markers can be both secreted or released from the tumour cells into the circulation by several mechanisms. These include proteolytic shedding of their extracellular domains, non-proteolytic cleavage of membrane anchors, alternative splicing resulting in secreted isoforms, and passive release due to cell death or membrane damage [7, 10]. Once in the extracellular space, these antigens can enter the bloodstream, where their concentrations can be measured and used as indicators of tumour presence or progression.

Various technologies have been developed for tumour marker detection. Immunoassays have long been a cornerstone of diagnostic testing, while nucleic acid–based methods such as hybridization and amplification have expanded clinical applications. More recently, techniques like liquid biopsy, single-cell sequencing, and advanced imaging have enhanced the ability to detect and monitor cancer progression [7]. Nonetheless, enzymatic immunoassays (EIA) and enzyme-linked immunosorbent assays (ELISA) remain the most widely used and validated platforms, with ELISA often considered the gold standard [8].

For accurate quantification, tumour biomarker assays rely on biological standards with known antigen concentrations. These standards serve as calibrators and controls in immunoassays to ensure consistent and reproducible results. Such standards can be derived from tumour cell lines, culture supernatants, recombinant protein expression systems, total protein lysates, or synthetic peptides. They must be appropriately purified to ensure specificity, stability, and precise quantification [8].

2.1.1 ZR75-1 and Its Antigens

ZR75-1 is an adherent human breast cancer cell line, established in the 1970s from the ascitic fluid of a 63-year-old woman with metastatic disease [11]. It grows as a monolayer and has a grape-like morphology, with a doubling time of around 80 hours at passage 40 [12].

ZR75-1 cells produce several tumour-associated antigens, including CA15-3, CA125, and CEA. These are harvested from the culture supernatant due to the release of the antigens from the tumour cell.

During culture, the expression of these antigens can vary, and CA125 often increases over time, reducing the relative abundance of CA15-3. At FDAB, CA15-3 is purified by precipitation from the harvested medium. Since CA125 and CEA are also present and co-precipitate, their relative levels may influence downstream assay specificity. However, the exact impact of this is still not fully understood. ZR75-1 cells are shown in Figure 2.1.

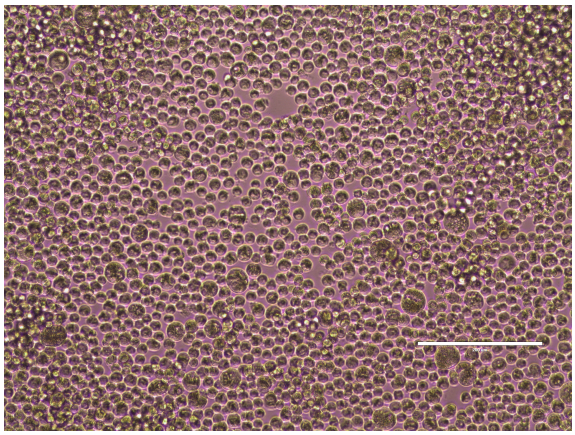

Figure 2.1. ZR75-1 cells in suspension. Image captured using the Invitrogen EVOS™ FL Imaging System.

2.1.1.1 Cancer Antigen 15-3

Cancer Antigen 15-3 (CA15-3) is a mucin-type glycoprotein derived from the MUC1 gene, which is overexpressed in many epithelial cancers. It is commonly used to monitor disease progression and response to treatment in breast cancer patients [13].

MUC1 is a transmembrane protein with a short cytoplasmic domain, a transmembrane segment, and a large extracellular domain composed of 20-amino acid tandem repeats heavily glycosylated with O-linked sugars [14]. In cancer, this protein is often overexpressed and aberrantly glycosylated, exposing otherwise hidden epitopes [15].

CA15-3 corresponds to the extracellular domain of MUC1, which is shed into the extracellular space via proteolytic cleavage by enzymes such as ADAM17 and MT-MMP1 [15]. Additionally, alternative splicing of MUC1 mRNA may generate soluble isoforms that lack the membrane-anchoring domain. These forms circulate in blood and culture supernatant and can be measured using immunoassays.

The immunoassay used in this study targets two epitopes: a sialylated carbohydrate epitope and an 8-amino-acid peptide sequence within the tandem repeat structure [16]. Elevated CA15-3 levels correlate with tumour burden, especially in advanced breast cancer, making it a valuable biomarker for clinical monitoring [13].

2.1.1.2 Carcinoembryonic Antigen

Carcinoembryonic antigen (CEA) is a 200 kDa glycoprotein with high carbohydrate content. It is part of the immunoglobulin superfamily, specifically the CEA-related cell adhesion molecules (CEACAMs), and plays roles in cell adhesion and migration [17, 18].

CEA is expressed in normal gastrointestinal mucosa and was first identified in colorectal cancer. It is now used as a non-specific tumour marker for gastrointestinal, lung, and breast cancers. In cancer, CEA is often overexpressed and released from the cell surface.

The release of CEA into the extracellular environment occurs through enzymatic cleavage of its glycosylphosphatidylinositol (GPI) anchor, as well as non-proteolytic mechanisms involving phospholipases [10]. These mechanisms generate soluble CEA that can be detected in cell culture supernatants and patient serum.

CEA levels in healthy adults are normally low but rise in malignancy. It is not specific enough for early diagnosis but is commonly used to track disease progression. The epitopes detected in the immunoassay used in this study correspond to Gold epitope IV and V [19].

2.1.1.3 Cancer Antigen 125

Cancer Antigen 125 (CA125) is a large mucin-type glycoprotein derived from the MUC16 gene. It is normally expressed during fetal development by coelomic epithelial tissues and is overexpressed in many ovarian cancers [17, 20].

CA125 is shed into the extracellular space through proteolytic cleavage of MUC16, and possibly also via alternative splicing and vesicular transport [21].

Multiple monoclonal antibodies such as OC125, M11, and OV197 recognize different protein epitopes within the core of CA125, enabling sensitive immunoassay detection [22]. In the assay used here, two independent epitopes on the protein core are targeted [23].

CA125 is a widely used marker for ovarian cancer monitoring but can also be expressed by other tissues, limiting its specificity. In ZR75-1 cultures, CA125 is also produced and quantified alongside CA15-3 and CEA.

2.2 Adherent Cell Cultivation Systems

This section explores the characteristics, culture techniques and bioreactor systems for adherent cells.

2.2.1 Cell Attachment Mechanisms

Mammalian adherent cells, also known as anchorage-dependent cells, are widely used in the production of biologics, vaccines, cell therapies and in tissue engineering applications [24]. Compared to microbial systems, mammalian cells offer advantages due to their ability to perform post-translational modifications and correct protein folding, making them essential for producing functional therapeutic proteins [25].

Adherent cells require attachment to a surface for growth and survival [26]. This process is one of the most important among higher life forms to create different tissues and organs [3]. Cell attachment is mediated by anchoring junctions, where transmembrane proteins link cells to either extracellular matrix (ECM) components or to neighboring cells.

Upon attachment to a surface, adherent cells undergo a series of morphological changes that can be divided into four general stages. Initially, cells make a weak, transient contact with the surface while remaining spherical. As adhesion progresses, the contact area increases and the number of bonds between the cell and the surface rises, although the cell still maintains a largely rounded shape. In the third phase, the number of attachment points temporarily decreases as the cell begins to spread, undergoing cytoskeletal rearrangement. Finally, in the fourth stage, the cells are fully spread out and firmly anchored to the surface, having established stable interactions with the surface through specialized adhesion structures such as focal adhesions [24].

Transmembrane proteins are crucial for the adhesion and spreading of cells [27]. Cell adhesion is dictated by the interaction of cell surface receptors, such as integrins and specific non-fibrous proteins naturally present in the ECM, like fibronectin, laminin and vitronectin. Integrins, composed of heterodimeric glycoproteins, are the most important cell surface receptors for cell attachment. These proteins bind to cell

adhesion proteins and collagen [24]. Divalent cations such as Ca^{2+} and Mg^{2+} are also required to stabilize these interactions [3].

Adhesion efficiency and cell growth are influenced not only by receptor-ligand interactions, but also by environmental factors such as medium composition, the presence of serum and the physical configuration of the culture system (e.g., static or agitated). Optimizing these parameters is crucial for achieving robust cell expansion in scalable systems [3, 27].

2.2.2 Development and Culture of Adherent Cells

The development of mammalian cell cultures begins with establishing a cell line. This can involve transfection with foreign genes or selection from natural populations based on desirable traits. Once a suitable clone is selected, it is expanded and cryopreserved in vials to create a master cell bank (MCB), which serves as a long-term source for all future production. Working cell banks (WCBs) are derived from the MCB for routine use in manufacturing. Vials from the WCB are thawed and expanded under standard culture conditions, typically at 37°C and 5–8% CO_2 in a humidified incubator [28].

Batch culture is the most fundamental cultivation mode, where all components, cells, nutrients and medium, are added at the beginning. The cellular growth in this process is characterised by four phases, lag phase, exponential phase, stationary phase and death phase. In the lag phase the cells are adapting to the new environment. The required time depends on the age of the inoculum and the previous environment. In production, the cells are already adapted to the culture environment and lag phase is minimal. In the following exponential phase, proliferation starts and cell density increases. In the stationary phase, the growth ceases and when energy sources and nutrients are depleted, the cells enter the death phase [28]. Batch culture is the most common practice for the following cultivation methods.

For small scale cultivation of adherent cell lines, petri dishes or multiwell plates are used where the cells can attach to the plastic surface. Larger tissue culture flasks (T-flasks) with surface areas from 12.5-225 cm^2 are used for growth and maintenance of cell cultures [29]. These sterile disposable plastic flasks provide a controlled environment where the cells can adhere [30].

When monitoring adherent cells in flasks, the confluency, which refers to the cell-covered area of the vessel, can easily be observed. This measure is used to determine when the cells should be passaged. Cell passaging is the process of transferring a part of the cells to a new cell culture vessel with fresh medium to promote continued cell growth. Because of the surface area restriction of adherent cell cultures, passaging timing is important to avoid overcrowding. Overcrowding can have several negative effects like changes in phenotype and induction of cell death. The type of cell line cultured determines the time between media change and passaging [31].

Scale-up cultivation is usually performed in roller bottles, which are cylindrical vessels that provide a dynamic system where incubation occurs under slow rota-

tion. The cells attach to the inner surface which is exposed to culture medium and gases while rotationally mixed. This prevents gradient formation of nutrients in the medium and gives a superior gas exchange [29, 30]. Roller bottles have a surface area between 500 and 1,700 cm^2. All maintenance in disposable flasks, like T-flasks and roller bottles, are labour intensive and cost-inefficient when working with larger cell numbers for production [29]

Spinner flasks, used in bench-scale cultures, are glass vessels equipped with a magnetically driven impeller. There is no surface for adherent cells to attach to, hence this needs to be provided in the form of microcarriers. Commonly, these flasks are used for initial cell cultures to test media and microcarriers before inoculation in bioreactors [29]. Spinner flasks can range in volumes from 100 ml to several liters [32]. The main advantages of spinner flasks is the mixing that improves aeration and gives a more homogenous nutrient supply. Additionally, a longer culture period can be achieved to generate higher cell numbers. The main drawback is the low oxygen transfer [29].

2.3 Bioreactor Culture

Large-scale production of mammalian cell-derived compounds, including vaccines, therapeutic proteins and diagnostic antigens, is typically performed in bioreactors. These systems range in size, from small bench-top reactors to industrial-scale units. The majority of animal cell cultures are operated in suspension, in batch or fed-batch mode. Perfusion cultivation is mainly applied for sensitive products. However, many established cell lines are anchorage-dependent, requiring surface attachment, unlike most cells in suspension cultures [28].

The stir tank bioreactor (STBR) is the most common type of reactor in industrial bioprocesses and for larger scales of mammalian cell cultures [29, 33]. The principle is the same as in spinner flasks but with greater control of exchange reactions [29]. The goal of the reactor is to create a homogenous environment for the cells where oxygen is evenly dispersed in the medium. STBRs are typically constructed from glass, carbonate or stainless steel and are equipped with an overhead motor that drives an internal impeller. In aerobic systems, a sparger is installed below the impeller to ensure even oxygen distribution throughout the culture. The impeller design can vary depending on the desired flow pattern inside the reactor. Reactors are also equipped with heat transfer devices, pH-meter, thermometer and dissolved oxygen sensor. The reactors are filled with 75-80% of the total volume to create a head space allowing gas exchange, foaming and mixing [33].

Bioreactor systems allow precise regulation of the physicochemical culture environment, in contrast to more basic vessels like flasks or spinner flasks. The parameters regulated in a bioreactor are commonly dissolved oxygen concentration (DO), pH, temperature, agitation and nutrient supply [32]. All these process conditions can be monitored online during the course of the culture [28]. The cell density in the reactor can be directly monitored online by optical probes or metabolic measurements or indirectly by oxygen consumption, carbon dioxide production, glucose consumption,

or lactate production [34]. Off-line sampling is also performed to directly monitor the cell density, metabolite concentration as well as other essential parameters [28]. The automated processes in bioreactors significantly enhance the efficiency and reproducibility of cell culture [32].

Early-stage development often favours flexible, batch-oriented systems to quickly generate material. In contrast, late-stage or commercial-scale operations prioritize robustness and reproducibility, typically relying on more controlled systems such as fed-batch or perfusion processes to ensure consistent product quality and yield [28].

2.3.1 Perfusion Culture

Perfusion culture is a type of continuous culture where fresh medium flows into the bioreactor and spent medium is removed at the same rate, but the cells are retained within the reactor. This method ensures that cells are continuously provided with fresh medium, preventing nutrient limitation, while the outflow removes by-products that could inhibit growth [28].

In perfusion culture, cell density increases as a result of the perfusion rate until a quasi-steady state is reached, maintaining a high cell density [30]. The process typically begins with a cell accumulation phase under optimized growth conditions to achieve as high cell density as possible. When the high density culture is achieved the production phase is initiated, where the reactor is operated during an extended period for consistent production [34].

Compared to other cultivation methods like batch, fed-batch and continuous, perfusion culture can achieve higher productivities [30]. This culture method is the most similar one to the physiology in the human body and is believed to provide a stable environment for mammalian cells [35]. A stable environment is important since the cells are producing a product, in the case of this project an antigen, and changes in environment can lead to physiological changes of the cells ultimately altering the biological products. Perfusion cultivation is widely used in production of biopharmaceuticals, such as monoclonal antibodies [36].

The media exchange can be explained by the dilution rate (D) which describes the volume per day. This is presented in Equation 2.1.

$$D = \frac{F}{V} \tag{2.1}$$

Where F is the volumetric flow rate and V is the bioreactor working volume.

Another variable developed for perfusion culture is the cell-specific perfusion rate (CSPR) presented in Equation 2.2 [34]. This parameter is used to create this constant environment for the cells based on the cell density of the culture.

$$\text{CSPR} = \frac{D}{X} \tag{2.2}$$

where D is the dilution rate and X is the cell density. CSPR helps optimize the perfusion process by ensuring that the nutrient supply matches the cell density, promoting high productivity and cell viability.

Efficient cell retention is critical for the success of perfusion cultures. The performance of a retention system can be quantified by:

$$\text{Efficiency} = \left(1 - \frac{\text{cell density in harvest}}{\text{cell density in bioreactor}}\right) \times 100 \tag{2.3}$$

Several technologies exist for cell retention. These include filtration, centrifugation, sedimentation and acoustic separation and may be implemented internally or externally to the reactor.

Filtration includes using cross-flow membrane filters utilizing a tangential flow to reduce fouling and spin filters that operates inside the reactor. The capacity of the perfusion is directly related to the surface area of the filter and when working with larger volumes, prevention of clogging the filter can become challenging [28]. To overcome this challenge, an alternating tangential flow (ATF) system connected to a hollow fibre filter can be implemented, enabling a back-and-forth flow to reduce fouling [36].

Different centrifugation methods can be used to separates cells based on density differences. Centrifugation is a way to enhance settling velocities and are effective for large-scale bioreactors due to their compact size and scalability. However, the high shear stress can affect cell viability [28].

Sedimentation uses gravity to separate cells and harvest medium. Cells, being denser than the medium, settle to the bottom while the clarified medium is drawn from the top. Two methods used are vertical and incline sedimentation, where vertical sedimentation exploits gravity to settle and separate cells in a vertical counter-flow, while inclined sedimentation enhances settling efficiency by using inclined tubes to improve cell separation. Since there is no filter used, it minimises the fouling and shear damage [28].

Ultrasonic resonators use acoustic waves to form loose cell aggregates, enhancing separation efficiency without damaging the cells, unlike mechanical separation methods. The acoustic waves create standing wave fields that aggregate cells based on their density and compressibility differences. The cell aggregates are retained inside the device while spent medium is pumped out [28]. Once the ultrasonic waves are turned off the aggregated cells sediment back into the reactor. Applikon BioSep (Getinge) is a ultrasonic separation chamber used for cell retention in this project. The system is developed for cell suspension, but microcarriers such as Cytopore and Cytodex can also be used together with the BioSep [3]. There is no reported usage of CultiSpher G microcarriers together with the BioSep. Ultrasonic resonators offer non-contact separation, reduced shear stress and minimal cell damage, making them ideal for high-density perfusion cultures and continuous bioprocessing.

2.3.2 Scale Up Considerations

Scaling up mammalian cell cultures involves replicating the physiological conditions of small-scale systems to ensure consistent growth and product quality. This involves maintaining optimal conditions for temperature, pH, dissolved oxygen, nutrient supply and waste removal [37].

For adherent cell lines, scale-up poses additional challenges due to their limited surface-to-volume ratio [30]. In monolayers of adherent cell lines, the cell number is directly proportional to the available growth surface. The limited surface area of culture vessels restricts the ability of cell proliferation. There are two main strategies to address this issue. Firstly, adherent cells can be adapted to grow as anchor-independent in suspension. This process is time-consuming and not all cells can be developed for this purpose. Also, the adaptation of the cells should not alter the production of the desired compound. Secondly, suspension culture systems could be utilized to imitate suspension conditions, which is a more commonly used approach [29]. One such method is the use of microcarriers, which provide a larger surface area for cells to grow on [38].

As scale increases, agitation and gas sparging rates must also be increased to maintain homogeneity and optimal dissolved oxygen and carbon dioxide levels. Key parameters for determining appropriate conditions include impeller tip speed, gas flow rate (VVM), power per volume (P/V) and the mass transfer coefficient (k_La) [37].

Oxygen is an essential component in cell culture since cells require a specific amount to maintain normal metabolism. It is provided either by exchange between the medium and head space gas in vessels, which often is improved by stirring, or in bioreactors by sparging of air or oxygen. Low oxygen levels lead to slower respiration, thus decreasing cell growth and product formation [29]. Sparged cultures achieve higher mass transfer rates of oxygen enabling higher cell densities. 50% air saturation is common in reactor cultures [34].

With bioreactors, the oxygen, nutrient transport and waste removal, enhance the culture. However, the agitation also exposes the cells to increased fluid shear stress. This stimulus can affect the growth of the cells in different ways. Shear stress has been shown to negatively affect cell viability, growth, and behaviour in many cases [29]. Sparging of cell cultures have also been shown to increase shear stress on the cells [34]. Adherent cells are more sensitive to shear stress than suspended cells [30]

Constant tip speed when scaling up is important to keep a consistent shear force, uniform mixing and consistent oxygen transfer. By maintaining this tip speed during scale-up, it is ensure that the mechanical environment remains consistent, which is crucial for the reproducibility and efficiency of the bioprocess. The tip speed (v_{tip}) can be calculated according to the following equation:

$$v_{\mathrm{tip}} = \pi \cdot d_{\mathrm{s}} \cdot n_{\mathrm{rpm}} \tag{2.4}$$

where d_s is the diameter of the impeller and n_{rpm} is the revolution per second of the impeller.

2.3.3 Culture Media

The environmental conditions for the *in vitro* growth of mammalian cells are carefully regulated to mimic their native physiological environment. These include a narrow range of pH, osmolarity, CO_2, O_2 and temperature. Essential components for a culture medium consists of water, salts, buffers, amino acids, vitamins and carbon source. The medium is commonly supplemented with animal serum for incorporation of important growth factors, hormones and other nutrients. Adherent cells often require more specific growth conditions than suspension cells. However, media containing serum usually provide a sufficient amount of ECM proteins, which support cell adhesion and proliferation. Calcium ions are particularly beneficial for adherent cell types, as they facilitate cell-substrate interactions [38].

Dulbecco's Modified Eagle Medium (DMEM), used in this project, is a widely used basal medium well suited for adherent mammalian cells. The feature of this medium is a high content of amino acids and vitamins required for growth [39]. DMEM is often supplemented with Fetal Bovine Serum (FBS), which is a frequently used serum in mammalian cell culture [24]. Serum is important since it contains vital components such as growth factors, hormones and adhesive molecules like fibronectin among others [25]. FBS was first introduced in the 1950s and has since then been used as a standard component in culture medium for mammalian cells in research, biotechnology and pharmaceutical manufacturing [40]. The composition of molecules on the microcarrier surface determines the type and amount of proteins adsorbed from the serum to the surface. This will in turn affect the adherence and proliferation of the cells. Adsorption of proteins from serum can both reduce and increase the cell attachment depending on the type of protein. Non-adhesive proteins reduce the cell attachment while fibronectin increases cell attachment. It has been shown that gelatin, which is the base of CultiSphere G, specifically binds fibronectin [24].

Despite its widespread use, FBS raises ethical and scientific concerns. It is derived from bovine fetuses during the slaughter of pregnant cows, leading to sustainability and animal welfare issues [41]. While FBS is widely used due to its compatibility with many cell lines, it is important to acknowledge the ethical concerns that follow. Additionally, there are scientific drawbacks to using FBS, such as its undefined nature, variability between batches and the risk of potential contamination [42]. Animal serum can contain contaminants like bacteria, mycoplasma and viruses [40]. Other drawbacks is that it is the most expensive component in culture media and contains a high protein concentration which can interfere with product purification.

An alternative is to use serum-free medium, which can provide a more consistent and defined environment for cell growth and eliminate ethical issues arising with FBS. Shifting from FBS to serum-free media would contribute to the 3Rs, replacement, reduction and refinement of animal experiments [40]

For a healthy cell growth, the cells should be fed with fresh media regularly to minimize occurrence of nutrient limitations and accumulation of metabolic by-products. By-products are commonly acidic, resulting in a pH drop of the media which often is indicated by a colour change [38]. DMEM contains phenol red, which transitions to yellow when the pH level drops below the optimal range [39]. Colour change is also used to detect contamination of the culture. Bacterial contamination is characterised by a transition of the medium from red to orange and ultimately yellow colour. Also, cloudiness of the medium that also can have a white film on the cell surface in the flasks dissipating when the flask is moved. When viewed under microscope at low power, bacteria can look like small black dots [43]. Regular monitoring and maintenance of the culture environment are crucial for optimal cell growth and contamination prevention. Observing colour changes and cloudiness in the medium, along with routine microscopic examinations, help ensure the health of the cell culture.

2.4 Microcarriers for Adherent Cell Culture

Microcarriers are small spherical beads that provide a supporting matrix for the growth of adherent cells in bioreactors and spinner flasks [2]. Their sizes typically range from 100–300 µm, with a buoyant density of approximately 1.03–1.04 g/ml [2, 30]. These properties enable adherent cells to be cultured in a suspension-like environment, facilitating higher cell densities while maintaining efficient control of pH, dissolved oxygen, nutrients and metabolite concentrations [24].

The use of microcarriers is especially advantageous in large-scale bioprocessing, including the production of vaccines (polio, influenza, rabies), monoclonal antibodies and stem cell therapies [24]. Cells attach to the surface of microcarriers and proliferate, forming a confluent monolayer, which significantly improves scalability and productivity [30].

Microcarriers can be used in different types of cell culture systems such as roller bottles, spinner flasks and bioreactors. STBRs have been utilized for cultivating a diverse range of microcarrier-supported cells and cells adapted to suspension growth, including hybridoma cells, Chinese hamster ovary (CHO) cells, baby hamster kidney (BHK21) cells, human embryonic kidney (HEK239) cells and others, with working volumes reaching approximately 10,000 liters [32].

2.4.1 Microcarrier Materials and Designs

Over the decades, significant advancements have been made in enhancing cell attachment to microcarriers. Various types of microcarriers have been developed to accommodate different cell types and diverse surface coatings have been created to improve cell recognition [24]. Microcarriers are broadly categorized into synthetic and natural polymer-based materials [2]. The choice of material plays a crucial role in cell attachment, growth and downstream processing. The surface of microcarriers determines the cellular interactions and surface hydrophobicity/hydrophilicity sig-

nificantly influences cell adherence, although the exact impact remains unclear [24].

Early microcarriers were primarily composed of synthetic polymers such as poly(lactide-co-glycolide) (PLGA), polyhydroxyethylmethacrylate, acrylamide, polystyrene and polyurethane [2]. While these materials provide mechanical stability, they lack essential ECM proteins, such as fibronectin and laminin, which are necessary for efficient cell adhesion. These adhesion molecules must either be incorporated into the microcarrier surface or supplemented in the culture medium. An important commercially available synthetic microcarrier is Cytodex ^{TM} 1 (Cytiva) which is based on a crosslinked dextran matrix, substituted with positively charged N,N-diethylaminoethyl (DEAE) for improved cell adhesion [3, 30]. Another polystyrene-based microcarrier is the Corning®Enhanced Attachment Microcarrier (Corning), coated to enhance hydrophilicity giving a negative surface charge to improve cell adhesion. A microscopic image of the Corning microcarriers can be seen in Figure 2.2.

Natural polymer-based microcarriers, such as those composed of gelatin, collagen and cellulose, are more biocompatible and resemble the ECM [44]. Many natural polymers contain RGD (Arg-Gly-Asp) tripeptide motifs, which facilitate integrin-mediated cell attachment [24]. The RGD tripeptide has been used to promote attachment of adherent cells in microcarrier cultures [30]. To fabricate natural microcarriers, animal-derived ECM can be used either as a coating or as the sole material [24]. This has been utilized by several manufacturers to improve the performance of microcarriers. Cytodex^{TM} 3 (Cytiva) has a dextran matrix coated with porcine collagen [3, 24]. An example of another important commercially available ECM-based microcarrier is CultiSpher G (Percell Biolytica) made purely of porcine gelatin and has been shown to support cell densities of 1×10^7 cells/ml with adequate oxygenation [45] [30]. Gelatin-based microcarriers, introduced in 1985, have since been widely used for a variety of applications [30] [46]. The porous structure of gelatin microcarriers increases the surface area further, compared to smooth beads. This can increase cell density and productivity. Figure 2.2 presents an image of CultiSpher G porous structure compared to the Corning microcarrier. The propagation inside the pores is also believed to shield the cells from shear stress occurring in stirred vessels [30]. Gelatin-based microcarriers are dissolved when treated with trypsin for cell detachment, which can facilitate subsequent procedures.

Another type of carriers tested in this project were BioNOC® II (ESCO Healthcare) and Fibra-Cel® Disk (Eppendorf), which are classified as macrocarriers. BioNOC II are 55×10mm strips made of polyester non-woven fabric [47]. Fibra-Cel Disks are made from a combination of polyester and polypropylene mesh. They are electrostatically pre-reated to enhance cell adhesion. The disks typically have a diameter of 6 mm. Even though the disks are designed for packed bed bioreactors, there are examples in the literature of other types of application [48].

The microcarriers used in this project are presented in Table 2.1.

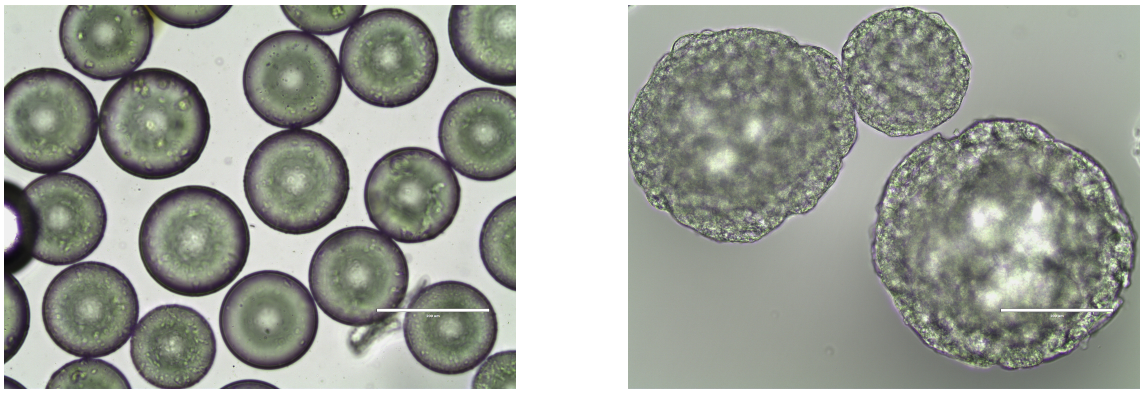

Figure 2.2. Left: Corning® Enhanced Attachment Microcarrier, a solid polystyrene-based carrier. **Right:** CultiSpher® G, a porous microcarrier composed of porcine gelatin. Images were taken using the Invitrogen EVOS^{TM} FL Imaging System.

Table 2.1. Material, structure, and size of the four microcarriers tested in this study.

Microcarrier	**Material**	**Structure**	**Size**
CultiSpher G	Porcine gelatin	Porous	130–380 µm
Corning Enhanced Attachment	Polystyrene	Solid	125–212 µm
BioNOC II	Polyester non-woven	Fibrous strip	3 x 10 mm
Fibra-Cel Disk	Polyester/polypropylene mesh	Fibrous disk	6 mm

2.4.2 Key Parameters for Optimizing Microcarrier Cultures

Optimizing microcarrier culture is crucial for maximizing cell yield, viability and reproducibility in large-scale bioprocesses [24]. Several factors influence cell attachment, growth and detachment, including microcarrier properties (surface chemistry and coating), seeding density and cell-to-bead ratio, bioreactor conditions (agitation, oxygenation and nutrient supply) and detachment and harvesting strategies.

Seeding conditions highly affect the cell attachment and is an important area for optimization. Inoculation is the most critical stage of the entire microcarrier culture [49]. Cells are prepared from a 2D culture by using proteolytic enzymes like trypsin to detach cells from matrix or detached from a previous microcarrier culture.

The phenomenon where cells attach to microcarriers is based on probability of interaction described by a Poisson distribution [24]. This is highly affected by the cell-to-bead ratio, where there should be enough cells to occupy all microcarriers. However, an excessively high ratio gives a high number of unattached cells. The optimal cell-to-bead ratio depends on the cell type [24]. When there is enough surface area available, the rate at which cells attach to microcarriers follows a first-order reaction pattern during the initial phase of attachment [50]. For CultiSpher G microcarriers the cell-to-bead ratio should be at least 10, up to 200 [45, 51]. For

Corning Enhanced Attachment Microcarrier the recommended cell-to-bead ratio is approximately 13 [52]. The microcarrier concentration in the seeding phase should also be considered. Different values between 1 g/L to 30 g/L have been reported, depending on the surface area of the microcarriers [24, 51, 52]. A high microcarrier concentration gives a great surface area but this must be weighed against the increased need for oxygenation and nutritional need. [24]

Stirring speed is a critical parameter in the cultivation of adherent cells on microcarriers. It influences cell attachment, distribution and overall culture performance. The primary goal during the cell attachment phase is to ensure that cells efficiently adhere to the microcarriers without being subjected to excessive shear stress, which can damage cells and reduce viability. Generally, a lower stirring speed is used during the attachment phase and a reduced culture volume (1/3 - 1/2) to maximize attachment [3, 51, 53]. Intermittent stirring is a commonly used practice to enhance attachment, used in many studies when expanding stem cells [24, 53, 54]. However, the study by Ng et al. showed that continuous stirring promoted better attachment of Vero cells on Cytodex 1, while CultiSpher G achieved higher attachment under intermittent stirring conditions [43]. On the other hand, continuous stirring is recommended by the CultiSpher manufacturer [51]. Hence, the cell type as well as microcarrier type dictated what the optimal attachment environment was. The attachment can be monitored by taking samples during the first hours after inoculation and comparing to the initial seeding density [55]. The percentage of cell attachment can be calculated according to the following equation:

$$\% \text{ Cell Attached} = (1 - \frac{\text{Cell density in medium}}{\text{Cell density at inoculation}}) \times 100 \tag{2.5}$$

The stirring speed commonly used when operating microcarrier cultures is the speed where the microcarriers are "just suspended", which can be referred to as N_JS [24]. Lower speeds can cause sedimentation and clumping of microcarriers and N_JS is highly dependent on the volume, vessel, impeller and microcarrier concentration. In a study evaluating 13 different types of microcarriers for human mesenchymal stem cell cultivation in 100 ml spinner flasks, N_JS was found to be 30 rpm [56]. In another study conducted by the same authors, the N_JS for a STBR was found to be 75 rpm with a 3-blade 45°-pitch wide blade impeller [57].

The critical steps with microcarrier cultures are the dissociation of cells from the carriers and harvesting cells from the culture media. A review from Bellani et al. reports the difficulty of efficient detachment of cells from the carriers in several studies [29]. While proteolytic enzymes are most commonly used to perform cell detachment, they can also cause cell damage [24]. Therefore, alternative methods are being developed, including the use of thermosensitive materials, cleavable surfaces on microcarriers and mechanical forces [24] [29]. Depending on the purpose of the culture, the detachment can be disregarded. In the case of this project, the cells only need to be detached for determining the cell density.

A study where CHO cells were grown on CultiSpher G in a 1 L stirred perfusion

reactor, showed that the cells do not occupy the interior of the microcarriers in the possible extent [50]. But the result still showed promising result of perfusion culture with macroporous microcarriers to obtain high density cultures.

Despite the extensive use of microcarriers in biopharmaceutical manufacturing, there is a notable gap in research specifically addressing the cultivation of ZR75-1 cells on microcarriers. This lack of research presents an opportunity to investigate and optimize microcarrier-based cultivation for ZR75-1 cells.

2.4.3 CA15-3 Production and Previous Microcarrier Research at FDAB

Currently, CA15-3 is produced in roller flasks. ZR75-1 cells are first thawed and expanded in T175 flasks before being seeded into 1 L roller flasks containing standard medium. The roller flasks are incubated for 3 weeks without medium exchange, following a death culture approach where cells grow until viability drops. A successful roller flask yields approximately 60 kU/L of CA15-3, though this varies between batches. As mentioned earlier, this method is labour-intensive due to the high number of flasks and large volumes of medium that must be handled manually. CA15-3 is obtained by precipitating the antigen from the harvested medium as a purification step. Other secreted proteins such as CA125 and CEA are co-precipitated. As a result, the relative antigen concentrations produced during culture could influence downstream assay specificity, however this is not fully known.

FDAB has conducted internal research on scaling up ZR75-1 cells using microcarriers, producing several findings that informed this thesis. In roller flask studies, microcarriers improved both cell viability and antigen productivity [58]. Among tested types, Cytopore 1 yielded the highest productivity, followed by CultiSpher S and G, while Cytopore 2 underperformed compared to controls. Simulated perfusion further enhanced productivity, peaking after two weeks, and the use of microcarriers helped prevent clumping, which otherwise reduced yields .

In "Proof of Principle" tests, sustained CA15-3 productivity was achieved over 50 days in a 10 L bioreactor using CultiSpher S, though cell growth was initially slow. Higher seeding densities improved output, eventually reaching levels comparable to 200 roller flasks. However, oxygen demand rose significantly at higher densities [59].

A nine-week feasibility study using batch, fed-batch, and perfusion phases confirmed that pre-culturing on microcarriers was unnecessary [60]. Optimizing carrier type, preparation, and applying alternating stirring during inoculation improved attachment and productivity .

Follow-up work reaffirmed the performance of Cytopore 1, and highlighted the importance of improved inoculation and sampling methods to ensure accurate measurements and nutrient distribution [61].

Finally, monitoring cell growth in roller flasks was challenging due to sampling limitations and difficulties counting cells on microcarriers. Several methods were

evaluated, but yielded inconsistent results [62].

Overall, these studies demonstrate the potential of microcarrier-based systems for CA15-3 production, while underscoring the need for optimized protocols and reliable analytical tools.

2.5 Enzymatic Immunoassay

Enzymatic immunoassays (EIAs) are versatile analytical tools used to detect and quantify a wide range of biological compounds and environmental contaminants. EIAs have a broad spectrum of applications and are essential in diagnostics for detecting antigens in the human body and critical antibodies in patient serum, aiding in disease progression monitoring. These methods offer advantages such as speed, sensitivity, selectivity and cost-effectiveness, making them suitable for large-scale sample analysis and rapid field testing. They are particularly useful when instrumental methods are impractical or too expensive, providing both quantitative and semi-quantitative results. Commercial testing kits are available for rapid testing [63].

The general process relies on immobilizing the analyte and using enzyme-labelled antibodies to produce a measurable signal, commonly colour changes indicating the presence of the target molecule. There are different types of EIAs, with enzyme-linked immunosorbent assay (ELISA) being a commonly used type in diagnostics [64].

FDAB has developed several EIA kits designed for the quantitative determination of specific antigens in serum. The technique is based on solid-phase, non-competitive immunoassays using the sandwich technique. Streptavidin-coated microplates are used together with biotinylated monoclonal antibodies (MAbs) to immobilize the antigen. The biotin-streptavidin system is often used to link proteins in different ways in immunoassays because of its strong bond, enhancing the sensitivity and specificity of the assays [64]. For detection, epitope-specific horseradish peroxidase-labeled MAbs are used to produce a measurable signal when a substrate for the enzyme is added. The enzyme catalyzes a reaction upon contact with the substrate, producing a colour change with intensities proportional to the antigen present in the sample. The absorbance of the colour change is measured to determine the antigen concentration.

The results are expressed in units per millilitre (U/mL), where unit is the measure of enzyme activity. It is defined as the amount of enzyme that catalyses the transformation of 1 micromole of substrate per minute under standard conditions [65].

3

Materials and Methods

This chapter describes the materials utilized, the procedures followed, and the analytical techniques employed to achieve the study's objectives.

The experimental procedure was structured into two parallel parts: spinner flask culture and bioreactor culture. Both systems were used to evaluate the feasibility of culturing ZR75-1 cells on microcarriers for CA15-3 production. Spinner flasks served as a flexible platform to evaluate microcarrier types, optimize attachment conditions, and monitor antigen production. In parallel, the bioreactor experiments focused on scaling up cultivation under controlled perfusion conditions, with attention to parameters such as stirring speed and oxygenation. An overview of the project is shown in Figure 3.1.

All cell handling was performed under a laminar airflow (LAF) hood, except when using the closed bioreactor system and during EIA procedures. Unless otherwise stated, all references to cell density refer to viable cell density. The ZR75-1 cell line used in this project was derived from a Working Cell Bank (WCB) at FDAB. The culture medium used, referred to as standard medium, consists of DMEM supplemented with FBS and other necessary additives.

3.1 Cell Expansion

A vial containing ZR75-1 cells (3×10^6cells/mL) was thawed and poured into a centrifuge tube containing 8 mL DMEM. The cells were centrifuged at 200 g for 5 minutes, and the supernatant was discarded. The cell pellet was resuspended in standard medium (DMEM with 20% FBS and 1% supplement). The suspension was transferred to a T75 flask (75 cm^2) and incubated at 37°C with 8% CO_2 for one week.

3.1.1 Cell Passaging

To further expand the culture, the cells were transferred to a larger T175 flask (175 cm^2) as follows: spent medium was discarded and the cells were rinsed with 7.7 mL PBS, which was then removed. Then, 7.7 mL trypsin-versene solution was added and gently swirled for 1 minute before being discarded. The flask was incubated at 37°C and 8% CO_2. After 10 minutes, the cells detached, and standard medium was

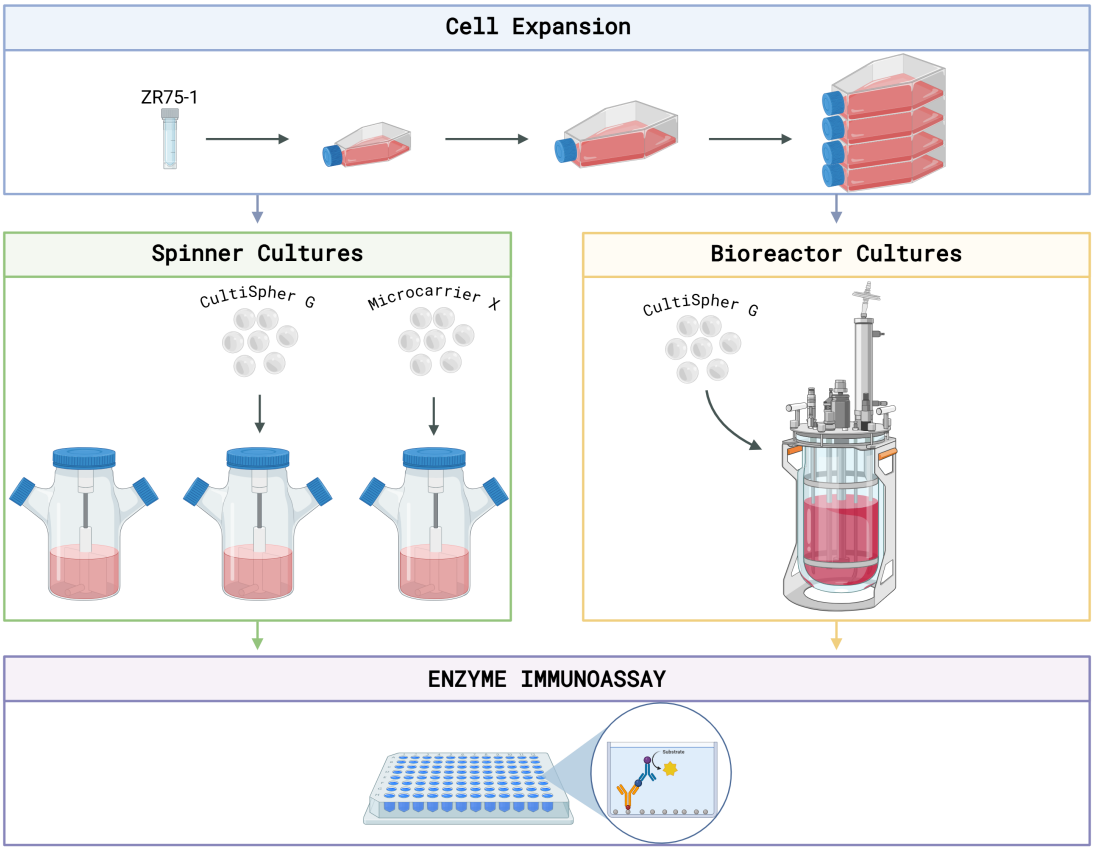

Figure 3.1. Overview of the experimental workflow used in this study. ZR75-1 cells were expanded in culture flasks and then seeded into spinner flasks or bioreactors containing microcarriers. Cultures were monitored for cell density, viability, and antigen production (CA15-3, CA125, and CEA) (created in https://BioRender.com).

added to stop the trypsin activity. The cell suspension was transferred into a new T175 flask and brought to 50 mL with additional standard medium (DMEM with 5% FBS and 1% supplement). The cells were incubated for one week.

Cells were further expanded from one T175 flask to four T175 flasks using the same procedure, with the trypsinized cell suspension equally divided among the new flasks. Cells were passaged weekly, and expansion to larger vessels followed the same protocol.

3.2 Cell Counting

To count the cell density of cells on Cultispher G microcarriers, 1 mL from the culture was pipetted into a 15 mL tube. After sedimentation of microcarriers, 0.9 mL of the medium was removed and 0.9 mL of trypsin-versene solution was added. The sample was incubated in 37°C for 30 minutes, or until microcarriers were dissolved. Occasionally, the sample was mixed to facilitate the detachment of cells. Two methods were used for cell counting: manual counting using a Bürker chamber

and automatic counting using a Cellometer™K2 (Nexcelom).

3.2.1 Bürker Chamber

A sample of the trypsinized cell suspension was loaded into the Bürker chamber and viewed under a light microscope. Cells within three A-squares were counted, following standard rules (include cells on the top and left boundaries). If the concentration exceeded 100 cells per A-square, the sample was diluted.

The average count, N, from the three squares was used to calculate cell concentration. The volume of an A-square is 1×10^{-4} mL. The formula used is:

$$\text{Concentration} = N \times F \times 10^4 \text{ cells/mL} \tag{3.1}$$

where F is the dilution factor.

Cell viability was calculated as the number of living cells divided by the total cell count.

3.2.2 Cellometer K2

The Cellometer K2 uses image cytometry to count cells and measure cell size. A sample of trypsinized cells was mixed with ViaStain™ AO/PI dye (20 µl cell suspension + 20 µl dye) in an eppendorf tube. Acridine Orange (AO) enters living cells and stains their DNA green, while Propidium Iodide (PI) stains dead cells red. The mixture was loaded onto a counting chamber and analyzed. The instrument provided cell density, size, and viability. A custom assay was developed to better match manual counts by adjusting image analysis thresholds.

3.2.3 Comparison of Cell Counting Methods

To evaluate the accuracy and reliability of the Cellometer K2 counting techniques for ZR75-1 cells, cell concentrations were measured using both the Bürker chamber and the Cellometer K2. A total of 22 samples were collected from various stages of culture in both spinner and bioreactor, and counted using both methods. Bürker counts were treated as the reference method.

3.3 Spinner Cultures

To evaluate cell growth and antigen production on a small scale, ZR75-1 cells were cultured on various microcarriers in 500 mL spinner flasks. Three flasks were used each round, one for each microcarrier type and one control without microcarriers.

The flasks were coated with Sigmacote (Sigma-Aldrich) to prevent cell attachment to glass. 20 mL of Sigmacote was added to each flask, swirled to coat, drained, air-dried in the LAF bench, rinsed with reverse osmosis (RO) water, and autoclaved.

ZR75-1 cells were pooled from T175 flasks to obtain enough cells. Each spinner was inoculated with 4.4×10^7 cells in 150 mL standard medium. Cell-to-bead ratio was 147 cells/bead. Microcarriers were prepared as described in Section 3.3.1 and added to the relevant flasks. Three rounds of spinner cultures were performed. The types of microcarriers used in each round of the spinner cultures, along with their respective concentrations, are summarized in Table 3.1.

Table 3.1. Microcarriers used in the three different rounds of spinner cultures

Microcarrier	Microcarrier Concentration	Round
CultiSpher G	1.0 g/L	1, 2, 3
Corning Enhanced Attachment	27.8 g/L	1
BioNOC II	16.7 g/L	2
Fibra-Cel Disk	20.0 g/L	3

The day after inoculation, spinners were topped up to 300 mL with standard medium. Stirring was set to 40 rpm throughout Round 1. In Rounds 2 and 3, stirring was set to 30 rpm on the first day and increased to 40 rpm thereafter. 40 rpm was estimated to $\mathrm{N}_J S$. Figure 3.2 presents a detailed representation of the method used.

Medium was exchanged twice per week. In flasks with microcarriers, the beads were allowed to settle and 150 mL of medium was removed and replaced. For the control flask, contents were poured into a 500 mL centrifugation tube and centrifuged at 200 g for 5 minutes. 150 mL medium was removed, the cell pellet was resuspended, transferred back to the spinner flask and topped up to 300 mL with fresh medium.

Samples were collected at each medium exchange for antigen concentration analysis using EIA for CA15-3, CEA, and CA125. Cell density and viability were measured in the CultiSpher G spinner flask. Images of cells and microcarriers was taken with Invitrogen EVOS^{TM} FL Imaging system.

The antigen productivity in the spinner flasks was calculated using Equation 3.2.

$$\text{Productivity} = \frac{C_i - \frac{C_{i-1}}{2}}{\Delta t} \tag{3.2}$$

C_i is the current antigen concentration (U/mL) in the spinner and C_{i-1} is the former antigen concentration. Δt is the number of days since the last medium replacement.

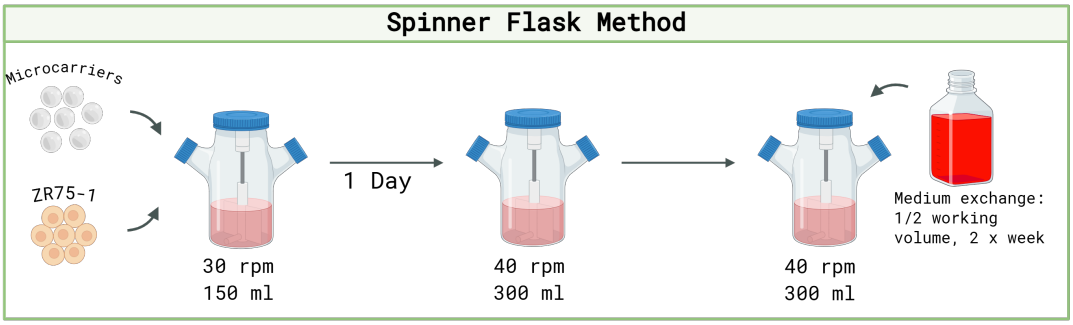

Figure 3.2. Overview of the spinner flask culture procedure in round 2 and 3. ZR75-1 cells were inoculated with 3 different types of microcarriers.

3.3.1 Microcarrier Preparation

Corning Enhanced Attachment microcarriers were prepared per manufacturer protocol [66]. 10 g of microcarriers was mixed with 100 mL sterile water. To achieve a concentration of 27.8 g/L in the spinner flask, 83.4 mL of this mix was transferred. After settling, the water was removed, and the beads were resuspended in 50 mL standard medium before being added to the spinner flask.

CultiSpher G microcarriers were prepared as recommended [51]. 1 g was rehydrated in 50 mL PBS for 1 hour in a 250 mL flask, then autoclaved and cooled. Autoclaved microcarriers were stored in the fridge. To obtain a 1 g/L concentration in the spinner flask, 15 mL of autoclaved microcarriers in PBS were transferred to a 50 mL tube for further preparation. After washing once with PBS and twice with medium, the carriers were transferred to the spinner flask. The tube was rinsed with additional medium to ensure full transfer to the spinner flask.

BioNOC II was prepared by weighing 5 g into a flask, covering with PBS, autoclaving at 121°C, and transferring the carriers aseptically with forceps. The PBS was removed and they were washed once with standard medium inside the spinner flask.

Fibra-Cel Disk was prepared by weighing 6 g and autoclaving them directly in the spinner flask with PBS. After cooling, the PBS was removed and replaced with standard medium. The flask was stirred at 100 rpm for 1 hour before inoculation.

3.3.2 Attachment Test

To evaluate the attachment kinetics of ZR75-1 cells to CultiSpher G microcarriers, an attachment test was conducted over a 23-hour period. ZR75-1 cells were harvested from T-flasks using trypsin-EDTA and counted using the Cellometer K2. A final concentration of 29.3×10^4 cells/mL was seeded into a spinner flask containing rehydrated and sterilized CultiSpher G microcarriers (1 g/L) and 150 mL of standard medium. The culture was maintained at 37°C with continuous stirring at 30 rpm.

To assess the attachment progress, 1 mL samples were withdrawn from the spinner flask at specific time points 1, 2, 3, 4, 5, 6, 7, 8 and 23 hours post-inoculation.

The supernatant containing unattached cells was collected and counted using the Cellometer K2. The attachment ratio was calculated by comparing the remaining cell density in the supernatant to the initial seeding concentration, according to Equation 2.5

3.4 Bioreactor Culture

Bioreactor cultures of ZR75-1 cells were conducted in a 3 L stirred-tank bioreactor (Applikon Bundle, Getinge) controlled by a Livit Flex unit. All bioreactor experiments used CultiSpher G microcarriers (Percell Biolytica), and cell retention was managed by the Applikon BioSep ultrasonic separation system. The reactor vessel was coated with Sigmacote as described in Section 3.3.

The ZR75-1 cells used were taken from the expanded cells in standard medium. The same medium was used throughout the bioreactor processes. Tubing and sensors were assembled prior to autoclaving. The optical DO sensor (Hamilton) was calibrated in water before autoclaving due to foaming in the medium. pH measurements were excluded due to a sensor malfunction, which was deemed acceptable for the purposes of this project.

All control parameters were managed by the Livit Flex control system to maintain a stable environment within the reactor, utilizing a PID controller to keep parameters at their set points. The monitored parameters included stirring speed, dissolved oxygen (DO), pH, temperature, and liquid level. The set points for temperature and DO were maintained at 37°C and 50%, respectively, throughout all experiments. Stirring was facilitated by a marine impeller with a diameter of 3 cm. Temperature regulation was achieved using a heating mantle surrounding the reactor, connected to the control system. Liquid level monitoring was performed during perfusion to maintain a consistent working volume.

The maximum tip speed from the spinner flask was translated to the bioreactor using Equation 2.4 to determine an appropriate stirring speed range.

Samples were regularly withdrawn from the reactor for determination of cell density, viability, and antigen concentration. Images of cells and microcarriers were taken with Invitrogen EVOS^{TM} FL Imaging system.

Antigen productivity was calculated using Equation 3.3 for batch mode and 3.4 for perfusion mode.

$$\text{Productivity} = \frac{C_i - C_{i-1}}{\Delta t} \tag{3.3}$$

C_i is the current antigen concentration (U/mL) in the reactor and C_{i-1} is the former antigen concentration. Δt is the number of days since the last sampling.

$$\text{Productivity} = C_i \times \text{F} \tag{3.4}$$

C_i is the current antigen concentration (U/mL) in the bioreactor and F is the perfusion rate (L/day).

Figure 3.3 presents an schematic representation of the different methods used, discussed in the method section below.

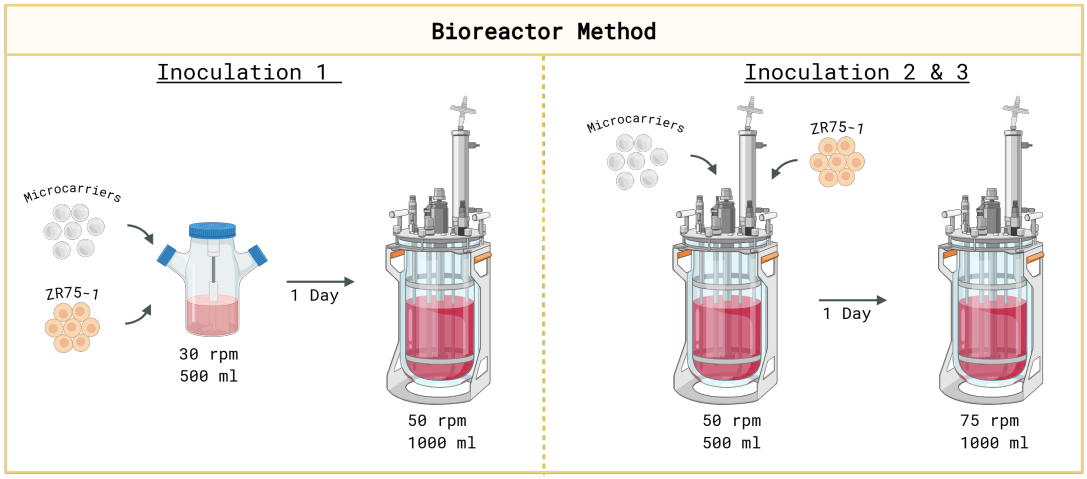

Figure 3.3. Overview of the two different inoculation strategies used for bioreactor cultures. In the first strategy (left), cells and microcarriers were pre-incubated in a spinner flask before being transferred to the bioreactor. In the second strategy (right), cells and microcarriers were added directly to the bioreactor (created with BioRender.com)

3.4.1 Bioreactor Inoculation 1

The initial attempt at bioreactor inoculation involved preparing ZR75-1 cells and microcarriers under controlled conditions to ensure successful cell attachment and growth.

3.4.1.1 Pre-Spinner Culture

Cells were first seeded in a 500 mL spinner flask for one day to pre-attach to the microcarriers. 1 g CultiSpher G was prepared according to the manufacturer's protocol [66] and added to the spinner flask. Cells harvested from 8 T75 flasks (totaling 1.5×10^8 cells) were transferred to the spinner and incubated at 37°C and 8% CO_2. The cell-to-bead ratio was 150. The next day, the entire content was transferred to a sterile inoculation flask with weldable tubing to allow aseptic transfer outside the LAF bench.

3.4.1.2 Inoculation and Culture

The pre-attached cell-microcarrier suspension was inoculated into the bioreactor with a working volume of 1 L. The culture was run in batch mode for the first five days. Stirring started at 30 rpm and increased to 50 rpm on Day 2 due to microcarrier sedimentation. On Day 4, stirring was increased to 60 rpm due to

clumping. On Day 5, 0.5 L of fresh medium was added to mimic fed-batch operation and support weekend culture. The increased volume also ensured that the level sensor was submerged (final microcarrier concentration: 0.67 g/L). Perfusion began on Day 7 at a flow rate of 0.43 L/day. However, a bacterial contamination was observed in the sample taken shortly after the perfusion start, and the culture was therefore terminated.

3.4.2 Bioreactor Inoculation 2

To reduce contamination risk, 1 g of CultiSpher G and 50 mL PBS were autoclaved directly in the bioreactor. 0.7 L of standard medium was added, and stirring was set to 100 rpm. Cells from four T175 flasks were pooled the next day. Cell density was measured as 2.97×10^6 cells/mL (Bürker chamber) and 2.25×10^6 cells/mL (Cellometer), totaling 35 mL or approximately 7.86×10^7 cells. Although this was half the previous inoculation concentration, it fell within the manufacturer's recommended range and was used. The cell-to-bead ratio was 78. The cell solution was transferred into an inoculation flask and inoculated in the bioreactor.

Stirring was initially set to 75 rpm for better microcarrier mixing and was estimated to N_JS. The working volume was 0.8 L for the first two days and was increased to 1 L on Day 3. Perfusion was started on Day 8 at 0.43 L/day (CSPR = 2.81 nL/cell/day). On Day 12, perfusion was increased to 0.65 L/day. Perfusion was stopped on Day 17, and batch operation continued until Day 27 when the culture was terminated.

3.4.3 Bioreactor Inoculation 3

2 g of CultiSpher G and 100 mL PBS were placed inside the bioreactor before autoclaving. After cooling, 0.5 L of standard medium with 100 ppm Antifoam C (Sigma-Aldrich) was added. Stirring and temperature were set to 150 rpm and 37°C, respectively.

The next day, cells from four T175 flasks were pooled to obtain 7.86×10^7 cells, which were inoculated into the reactor. The cell-to-bead ratio was 39. Stirring was initially set to 50 rpm. After 24 hours, it was increased to 75 rpm, and the volume was raised to 1.1 L due to an incorrectly adjusted level sensor. Perfusion was never started in this culture since high enough cell density was not reached and the culture was terminated.

3.5 Enzymatic immunoassay

Enzymatic immunoassays (EIAs) were used to quantify the concentrations of CA15-3, CA125, and CEA antigens in the culture supernatants. All EIAs followed validated protocols provided by FDAB [16, 19, 23]. Detailed procedures for each assay are available in Appendix A.

Each EIA is a solid-phase, non-competitive immunoassay using a sandwich format. For each antigen, samples and calibrators were incubated with: a biotinylated monoclonal antibody (MAb), an HRP-conjugated monoclonal antibody and streptavidin-coated microstrips for antigen immobilization.

The antigen-antibody complexes were detected using TMB (3,3',5,5'-tetramethylbenzidine) substrate, which reacts with HRP to produce a colour change. Absorbance was measured at 620 nm using a plate reader. Results were presented in U/mL and compared to calibration standards to quantify antigen concentration.

3.6 Statistical Analysis

All statistical analyses were performed using Microsoft Excel. Antigen concentrations between different conditions were compared using a two-tailed Student's t-test with a significance threshold of $p < 0.05$. Cell counting methods were evaluated using linear regression and paired t-tests to assess correlation and significance.

4

Results and Discussion

This chapter presents the outcomes of the experiments conducted to evaluate microcarrier-based cultivation of ZR75-1 cells for antigen production. Results from spinner flask and bioreactor cultures are analyzed with a focus on cell growth, viability, and productivity of CA15-3. The findings are discussed in relation to process scalability, microcarrier performance, and implications for future optimization.

4.1 Evaluation of Microcarriers for Spinner Flask Cultures

The spinner flask experiments were conducted to evaluate the growth and antigen production of ZR75-1 cells cultured with and without microcarriers. Three rounds of cultures were performed, testing different microcarrier types and conditions. The results include comparisons of CA15-3 productivity, cell density, viability and attachment efficiency.

4.1.1 CultiSpher G Outperforms Other Microcarriers in CA15-3 Production

The initial objective was to evaluate the suitability of different microcarriers for the cultivation of ZR75-1 cells and the production of CA15-3 antigen. CultiSpher G, Corning Enhanced Attachment, BioNOC II and Fibra-Cel Disk microcarriers were compared.

Three rounds of spinner flask cultures were conducted. The first round was terminated on day 8 due to bacterial contamination in all spinner flasks, thus only providing data from day 5. In the second round, the BioNOC II culture was terminated early on day 2 due to contamination. The CultiSpher G spinner was terminated on day 15 and the reference culture on day 18, both due to infection. In the third round, the Fibra-Cel Disk spinner culture was terminated on day 16 for the same reason.

Frequent contamination reduced usable data and highlighted the challenge of maintaining sterility during long-term spinner cultures with regular medium exchange. From the failed cultures, it can be concluded that BioNOC II and Fibra-Cel Disk

are not suitable for spinner flask cultivation. In both cases, the carriers did not remain evenly distributed during agitation. Instead, they became stationary within the flask, likely contributing to reduced mixing and poor culture performance.

From the first round of spinner culture, a slight increase in CA15-3 productivity was observed with CultiSpher G compared to the Corning Enhanced Attachment Microcarrier after 5 days, as can be seen from the results presented in Table 4.1. However, when comparing these results with a Student's t-test, this difference was not statistically significant, with a p-value of 0.16. Therefore, further replicates are needed to assess possible differences between the Corning and CultiSpher G microcarrier.

Table 4.1. CA15-3 productivity measured on day 5 in two ZR75-1 spinner flask cultures with different microcarriers. Values are based on two replicates. No statistically significant difference was observed ($p = 0.16$).

Microcarrier	**CA15-3 Productivity** (Mean ± SD, U/mL)
Corning Enhanced Attachment	5.66 ± 0.01
CultiSpher G	6.02 ± 0.13

In the third round of spinner flask experiments, CultiSpher G performed better than both the reference culture and Fibra-Cel Disk in terms of CA15-3 antigen production as shown in Figure 4.1. The CultiSpher G culture remained viable until the experiment was terminated at day 28 and showed steadily increasing productivity, peaking near the end of cultivation. Fibra-Cel Disk cultures produced significantly lower CA15-3 levels than CultiSpher G at all measured time points, with particularly low values after day 13. Fibra-Cel Disk cultures demonstrated inferior performance compared to both CultiSpher G and the reference during the measured days.

Statistical comparison, using Student's t-tests, between CultiSpher G and the reference showed no significant difference at early time points (day 5 and 9). However, from day 13 and onward, the differences became statistically significant ($p < 0.05$). This indicates that while initial productivity levels were comparable, the CultiSpher G microcarrier supported prolonged and enhanced antigen production as the culture matured. CA15-3 concentrations and statistical significance testing between conditions can be found in Appendix Table B.3 and Table B.4.

The results support the conclusion that CultiSpher G is the most effective microcarrier tested in this study for ZR75-1 cultivation and CA15-3 production. Its performance surpasses both Fibra-Cel Disk spinner and the reference, making it a promising candidate for future scale-up in bioreactor systems. These results also support that antigen production increases when cells are grown on a surface.

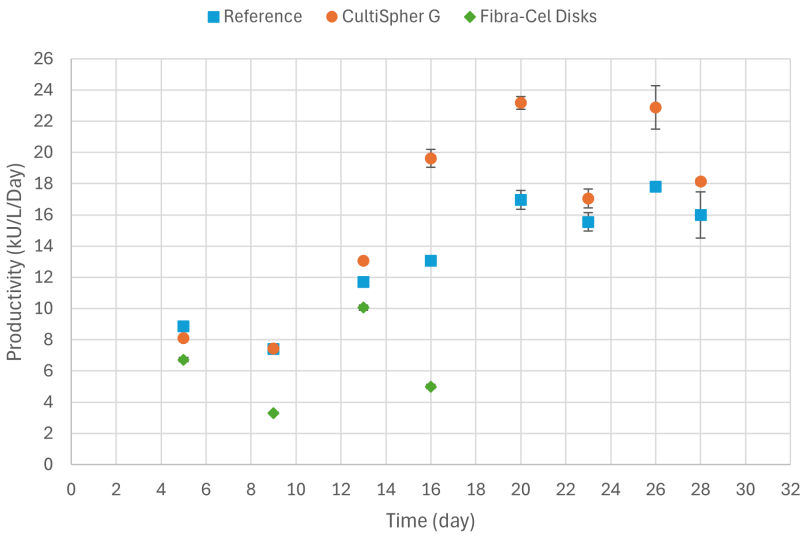

Figure 4.1. Comparison of CA15-3 productivity in the third round of spinner flask cultures using CultiSpher G, Fibra-Cel Disk and a reference culture. The CultiSpher G culture showed consistently higher antigen production over the 28-day period. Fibra-Cel Disk cultures were terminated on day 16 due to contamination. Error bars indicate the standard deviation (n=2)

4.1.2 High Viability and Productivity of ZR75-1 Cells on CultiSpher G

The cell density and viability were measured in the CultiSpher G spinner flask only. Attempts were made to count cells in the other spinner flask, but detachment of the cells from the other types of carriers was more difficult. Since CultiSpher G is degradable by trypsin, the solution could be treated as a suspension, which simplified measurements of cell density and viability. The cells in the reference flask contained clumps of cells and representative samples could therefore not be collected.

The CultiSpher G microcarriers spinner in the third round was monitored for both viable cell density and cell viability over the 28-day period presented in Figure 4.2. The initial viable cell density was approximately 15×10^4 cells/mL, which slightly decreased by day 5. The density increased with a peak at day 16 (1.17×10^6 cells/ml) and then declined but maintained an overall upward trend. The viability in the CultiSpher G culture stayed above 80% for the entire culture. The cell density data is available in Table C.1 in Appendix C.

The consistently high viability indicates that most cells remained metabolically active, supporting the potential for extended cultivation and scale-up. The twice-weekly medium exchange likely provided sufficient nutrients and waste removal, helping maintain cell health and preventing build-up of inhibitory by-products. These results highlight how regular medium exchange mimics perfusion, supporting sustained viability and productivity.

The sharp increase at day 16 seen in Figure 4.2 could be due to chance, since more

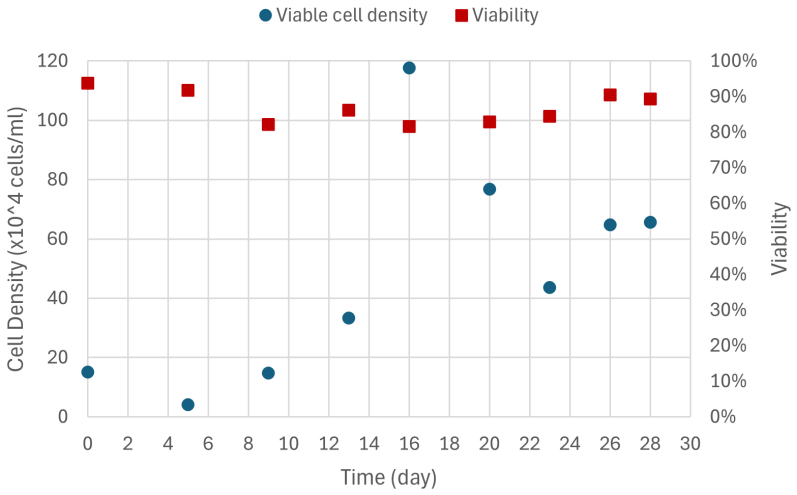

Figure 4.2. Viable cell density and cell viability over 28 days in the third CultiSpher G spinner culture. A peak in cell density is observed around day 16, while viability remained above 80% throughout the culture period.

densely populated microcarriers might have been sampled. Another explanation for the peak could be that the culture reached its maximum density that could be supported by the available surface area, or that localized nutrient or oxygen limitations restricted further cell expansion. Overcrowding of cells on a surface can lead to a decline in growth and has been seen in microcarrier cultures [31] [67]. However, due to the porous structure of the microcarriers, it was difficult to visually assess the extent of cell attachment and distribution. Therefore, it is not possible to determine whether overcrowding occurred in this culture.

Figure 4.3 shows the cells on microcarriers at day 28 of the CultiSpher G culture. Compared to Figure 2.2, which shows CultiSpher G without cells, a visible difference can be observed in how light passes through the carriers. In Figure 4.3, some areas of the microcarriers appear darker, indicating a higher density of attached cells. Other microcarriers appear more unoccupied. The smaller dark clumps seen in the image are likely cells that have spontaneously aggregated. Similar clumps were also seen in the reference flask, presented in Figure 4.4.

To evaluate the efficiency of microcarrier use in this culture, an estimate of microcarrier occupation was made. According to the manufacturer, one gram of CultiSpher G contains approximately 10^6 microcarriers, each capable of supporting 2,000–3,000 cells [45]. In this experiment, 1 g/L was used in a 300 mL culture volume, corresponding to 300,000 microcarriers. The maximum cell number at peak density of 1.17×10^6 cells/mL implies approximately 1,170 cells per bead. This is a significant increase to the approximately 147 cells per bead that were seeded. Visual inspection suggested that a substantial number of microcarriers remained unoccupied, as seen in Figure 4.3, indicating that the cells may have been unevenly distributed. It is possible that the microcarriers that were occupied had become overcrowded. This uneven distribution could be the result of inefficient cell attachment during inocu-

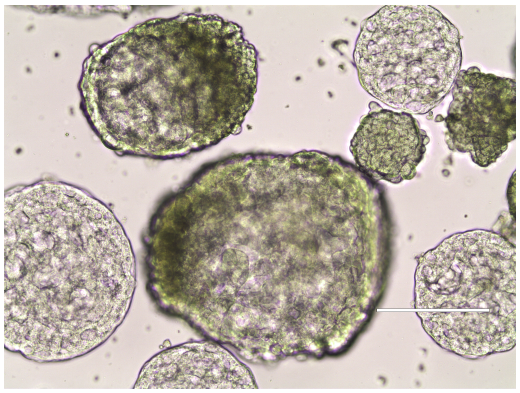

Figure 4.3. CultiSpher G with cells on day 28. Darker regions indicate areas of higher cell attachment.

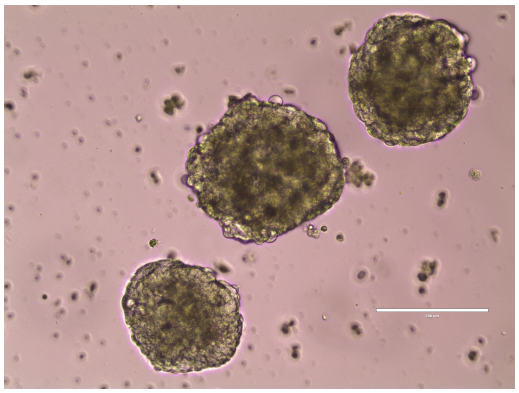

Figure 4.4. Reference culture on day 28. Visible dark aggregates indicate spontaneous cell clustering.

lation or due to spontaneous aggregation of cells, which would prevent a more even spread across the microcarriers.

When comparing these results to other studies using CultiSpher G in spinner flasks, it becomes evident that ZR75-1 cells reach a lower density than some commonly used cell lines. For example, CHO-K1 cells have reached 6×10^6 cells/mL after 14 days at 0.5 g/L microcarrier concentration [68] and HepZ cells reached 4.5×10^6 cells/mL after 7 days at 1 g/L and 30 rpm stirring [69]. Vero cells have also achieved 1.4×10^6 cells/mL under similar conditions with an estimation of over 1400 cells per bead [43], which is similar to the result obtained in this study. Even though the cell lines differ and the growth rates can't be compared, these results still give a good indication of the expected number of cells that can occupy the microcarriers. Based on this, there is room for further optimization of the ZR75-1 cell culture parameters, but the results show that the cells are able to successfully grow and remain viable on CultiSpher G microcarriers over an extended cultivation period.

Overall, these results demonstrate that CultiSpher G is a suitable microcarrier for supporting ZR75-1 cell growth over prolonged periods. The combination of high viability and increasing cell density indicates that this system may be optimized further for increased antigen productivity, for example, by increasing microcarrier concentration, adjusting feeding frequency, or implementing full perfusion in a bioreactor setting.

4.1.3 CA15-3 Productivity in CultiSpher G Exceeds Roller Production

The productivity of CA15-3 in both the spinner culture and the current roller bottle process is presented in Figure 4.5. The roller bottle culture, used at FDAB, is a batch system with an estimated constant productivity of approximately 8.6 kU/L/day. This estimation is based on weekly harvests and an assumed antigen concentration of 60 U/mL.

The productivity in the CultiSpher G spinner increased gradually throughout the culture, peaking on day 20 at around 23 kU/L/day, followed by a slight decline towards the end. This trend follows the cell density and viability data presented in Figure 4.2, where the peak productivity occurred after the period of highest viable cell density. Even though the viable cell density decreased after day 20, the productivity remained relatively high, indicating that the ZR75-1 cells continued to produce antigen despite a reduced rate of proliferation. This suggests that once the cells are established, they can maintain productivity even in later phases of the culture.

Initially, both spinner and roller systems exhibited similar levels of productivity. In the roller bottle process, cells begin producing antigen early in the culture period, but without medium exchange, nutrient levels decline. As a result, cell viability drops, leading to a gradual reduction in productivity over time.

In contrast, the spinner culture using CultiSpher G supported sustained cell growth and productivity beyond the early phase. Medium exchange allowed for replenishment of nutrients and removal of waste, enabling cells to remain viable and active. Peak productivities in the spinner system reached up to 23 kU/L/day and remained consistently above 15 kU/L/day after day 13. This represents a significant improvement, with the highest productivity showing an approximate 167% increase compared to the roller culture.

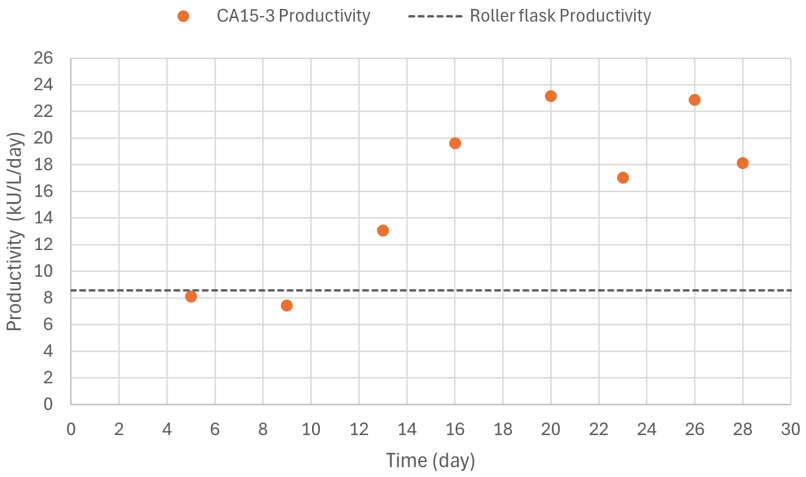

Figure 4.5. CA15-3 productivity over time in the CultiSpher G culture compared to the estimated constant productivity of the roller bottle process (8.6 kU/L/day). Productivity in the spinner culture increased gradually and peaked at day 20, with values remaining above 15 kU/L/day after day 13.

The earlier comparison of microcarriers showed that the reference culture produced less CA15-3 than the CultiSpher G culture (Figure 4.1). Combined with the previous discussion on spontaneous cell aggregation, this supports the idea that a more even distribution of cells on microcarriers could enhance both growth and productivity even more.

Together, these results highlight the potential of CultiSpher G to support efficient CA15-3 production, while also pointing to the need for further optimization of the inoculation process to improve microcarrier occupation and overall productivity. Microcarrier cultivation can also exceed the roller bottle method in terms of antigen yield, particularly during the later stages of cultivation.

4.1.4 Attachment Efficiency of ZR75-1 to CultiSpher G

Attachment kinetics of ZR75-1 cells to CultiSpher G microcarriers were assessed over 23 hours by sampling unattached cells in the medium. Minimal binding occurred within the first 2 hours, with 38% attachment at 3 hours. Attachment increased steadily to 65% by 8 hours and reached 89% at 23 hours, which can be seen in Figure 4.6. This gradual adhesion is consistent with the multi-phase nature of cell attachment [3, 24]. Attachment data can be found in Appendix C.

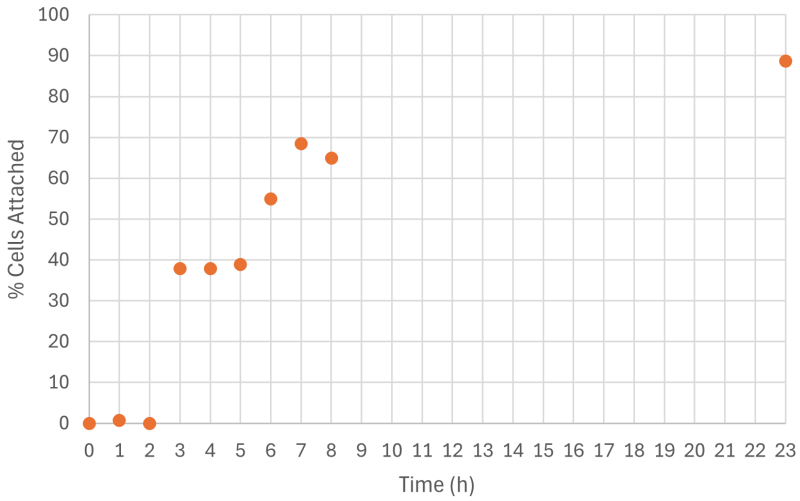

Figure 4.6. Attachment kinetics of ZR75-1 cells to CultiSpher G microcarriers over 23 hours.

Despite high final attachment, early clumping was observed and likely limited even microcarrier occupation. This aggregation behavior has been observed for ZR75-1 during the study and may reduce initial adhesion efficiency.

Continuous stirring at 30 rpm may have contributed to suboptimal early attachment, either by reducing contact or causing mild shear. Literature shows that intermittent stirring improves attachment rates in other cell types, with 90% attachment seen within 130 minutes for Vero cells on CultiSpher G [43]. Another study using hBM-MSCs reported 55% attachment to CultiSpher G after just 1 hour under both static and agitated conditions [56]. This indicated that ZR75-1 cells exhibit slower adhesion kinetics but also that different attachment conditions should be explored.

These results suggest that early ZR75-1 attachment is slower and may benefit from adjusted inoculation conditions, such as intermittent stirring or higher seeding density, to reduce aggregation and enhance distribution. Cell aggregation within the

first hours may limit the effective use of microcarriers. Once aggregates form, cells may become less likely to spread out and attach uniformly, a pattern that aligns with the observed presence of large cell clusters and many unoccupied microcarriers in the spinner flask. This likely leads to local overcrowding on some carriers while others remain unused. Improving early cell distribution could enhance microcarrier utilization, supporting better cell growth and increased antigen productivity.

While ZR75-1 cells did reach a satisfactory attachment ratio on CultiSpher G, comparison to other studies shows that attachment can be faster under different conditions. This underscores the importance of tailoring the inoculation and stirring protocols specifically for ZR75-1 to maximize microcarrier occupation and downstream productivity.

4.1.5 Comparison of CA15-3, CA125 and CEA Production

The antigen production in the third round of spinner culture was monitored for 28 days in both the CultiSpher G and the reference cultures. Figure 4.7 and Figure 4.8 show the accumulated quantities of CA15-3, CA125 and CEA in kilo units (kU).

In both cultures, CA125 was the most abundantly produced antigen, followed by CA15-3 and CEA. In the CultiSpher G culture, CA125 reached over 500 kU by day 28, while CA15-3 reached approximately 120 kU and CEA about 60 kU. In contrast, the reference culture accumulated approximately 190 kU of CA125, 110 kU of CA15-3 and 60 kU of CEA.

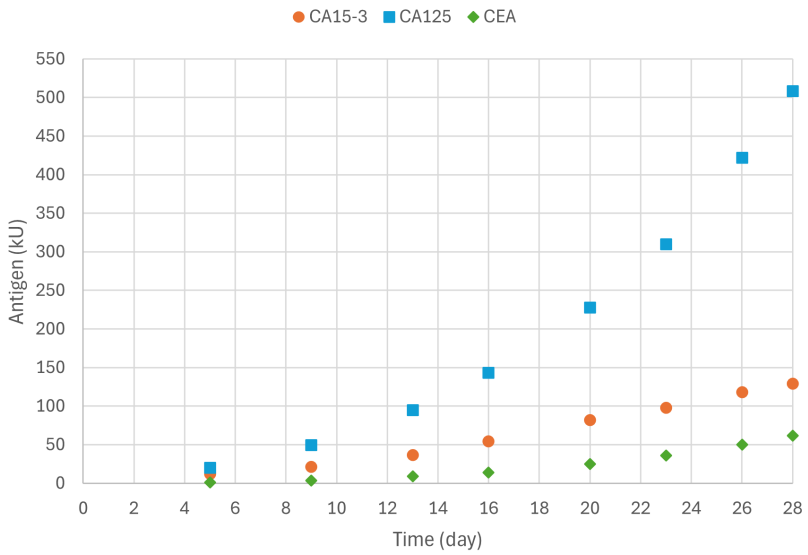

Figure 4.7. Accumulated antigen production of CA15-3, CA125 and CEA over 28 days in the CultiSpher G spinner culture. CA125 was the most abundant antigen, followed by CA15-3 and CEA.

These results show that antigen production was higher overall in the CultiSpher G culture. CA125 accumulation in the CultiSpher G culture significantly exceeds that

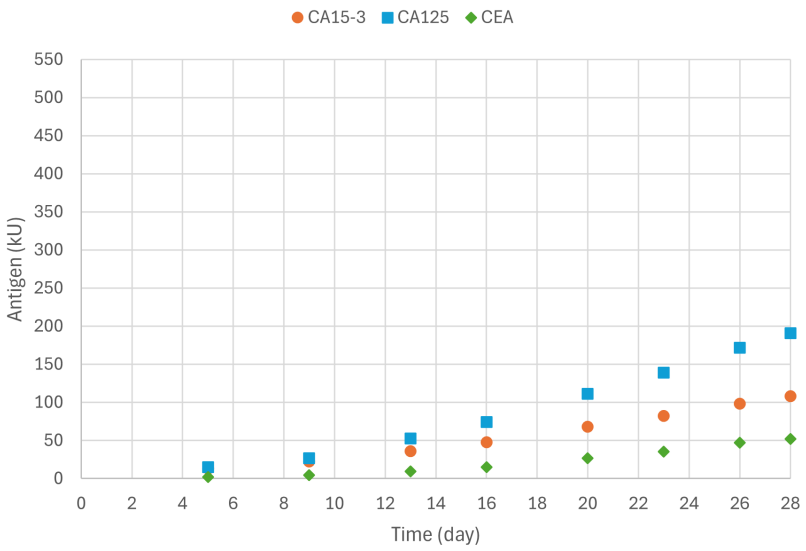

Figure 4.8. Accumulated antigen production of CA15-3, CA125 and CEA over 28 days in the reference spinner culture. CA125 was the most abundant antigen, followed by CA15-3 and CEA.

in the reference culture. While the ratio between the antigens changed somewhat over time, CA15-3 remained stable or increased throughout, suggesting that the production of CA125 and CEA did not occur at the expense of CA15-3. There is some concern that increased expression of other antigens could reduce CA15-3 yield. However, that does not seem to be the case under these conditions.

From a process development perspective, the elevated levels of CA125 could have implications for downstream processing. To isolate CA15-3, the antigen is typically precipitated and high concentrations of CA125 might interfere with this step, either through co-precipitation or by competing during recovery. In the current roller bottle production at FDAB, CEA is usually present at around 12 kU/L at the end of the culture. If alternative systems produce higher levels of CA125 or CEA, it could potentially complicate purification and impact final product purity, depending on which antigen is targeted. But the effects of this is not known and there might as well not be a problem with higher CA125 and CEA levels.

4.2 Scale-Up to Bioreactor Reveals Challenges and Potential

The aim of the bioreactor cultures was to evaluate if the ZR75-1 cell line could be successfully scaled up using CultiSpher G microcarriers and integrated into a stirred-tank bioreactor (STR) system with or without perfusion.

4.2.1 Bioreactor Culture 1

Bioreactor culture 1 operated in batch mode for 7 days and the CA15-3 concentration in the reactor reached 55 U/mL, corresponding to a productivity of 5.3 kU/L/day. The Livit Flex bioreactor parameter trace, showing dissolved oxygen (DO), temperature, air, and oxygen addition over time of this run is presented in Appendix D Figure D.1.

The culture was terminated due to an infection of presumably rod-shaped bacteria with an unknown origin. During one step in the inoculation, there was leakage from the tubing, which could be a cause, but a more likely explanation is that the culture flasks pooled to inoculate the reactor already had an infection not noticed.

Conclusions from the first inoculation was that the medium was foaming a lot when the culture was supplied with air through the sparger. Hence the DO sensor should be calibrated in water prior to autoclaving. The microcarriers were accumulating in the foam and stuck to the walls of the vessel when the foam decreased. Also, when starting perfusion at the desired rate, the pump was not strong enough to push the medium through the tubing. This was much likely due to clumps of microcarriers blocking the tubing connected to the BioSep port, which was observed when the culture was terminated. To prevent this issue, no tubing should be connected to the BioSep.

4.2.2 Bioreactor Culture 2

Bioreactor Culture 2 ran for 27 days, with perfusion starting on day 7 and ending on day 17. A total of 5.4 L of culture medium was harvested during this period. Microcarrier concentration in the harvest was estimated at less than one per mL, indicating that the BioSep system efficiently retained them. Data from this run is presented in Appendix D.

Figure 4.9 shows the viable cell density and viability over time. Cell density dropped sharply after perfusion began and did not recover until perfusion stopped. Viability remained above 80% for most of the culture but dipped briefly to 50% after perfusion ended.

Antigen concentrations of CA15-3, CA125 and CEA in the bioreactor are shown in Figure 4.10. As with cell density, antigen levels declined during perfusion and recovered afterwards. This suggests that the perfusion rate exceeded the culture's production capacity, leading to a washout effect. Once perfusion stopped, antigen concentrations increased, aligned with the recovery in cell density. This indicates that the antigen production is directly tied to the viable cell population.

These results suggest that perfusion may have been initiated too early, before the culture reached a sufficient cell density. The cell separation system, which circulates the microcarriers through tubing, may also have exposed the cells to excessive shear stress reducing the cell density. This type of mechanical stress has previously been observed to negatively affect other cell cultures at FDAB. A possible solution is to use a more gentle pump head to reduce the impact on the cells.

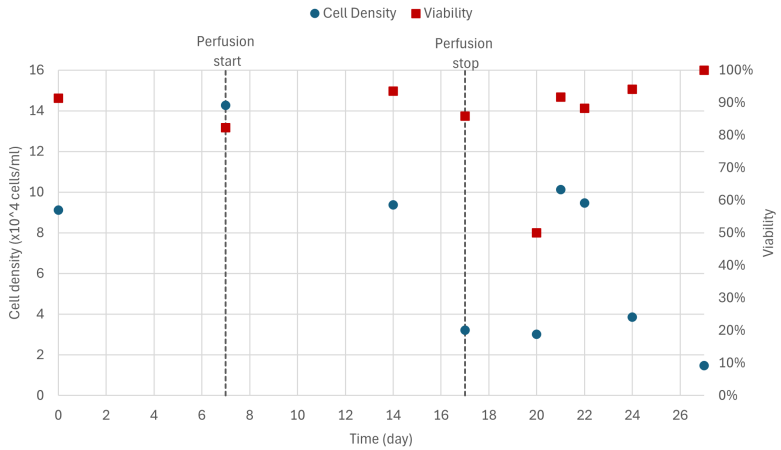

Figure 4.9. Viable cell density and viability over 27 days in bioreactor culture 2. Perfusion started on day 7 and stopped on day 17. Cell density decreased during perfusion but recovered afterwards. Viability remained above 80% for most of the culture, except for a brief drop after perfusion ended.

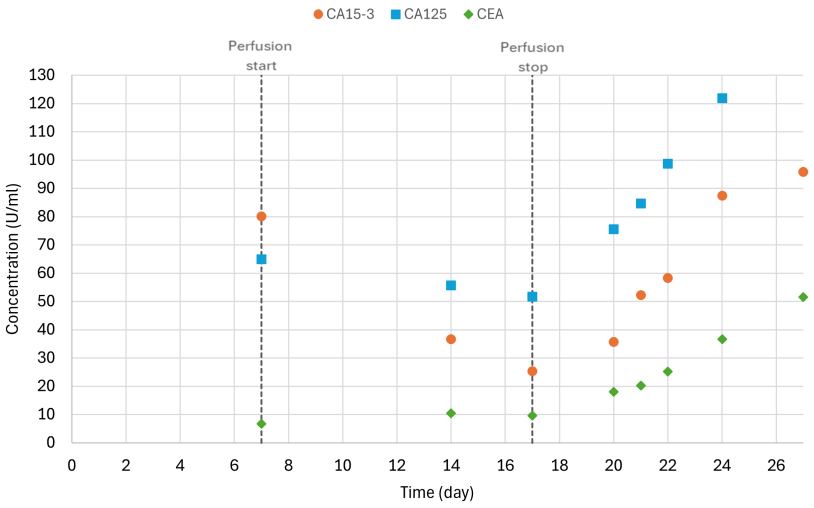

Figure 4.10. Antigen concentrations of CA15-3, CA125 and CEA in bioreactor culture 2 over time. Levels declined during perfusion (day 7–17) and increased again after perfusion stopped, in line with the recovery in cell density.

The perfusion rate of 0.43 L/day was the minimum setting for the pump, but in a 1 L working volume, this may have been too high. A larger culture volume could reduce the relative turnover, lowering shear and washout risk. 0.43 L/day was initially used but when cell density dropped it was increased to 0.54 L/day to see if cells required more nutrients, which was not the case.

CSPR values highlight this imbalance. On day 7, the bioreactor culture had a CSPR of approximately 5300 pL/cell/day, reaching over 16,000 pL/cell/day by day 14. In contrast, spinner cultures ranged between 100 and 3100 pL/cell/day, decreasing as the cell density increased over time. The higher CSPR in the bioreactor likely caused overfeeding and antigen dilution. A full table of CSPR values is included in Appendix E.

Oxygen addition increased notably after perfusion stopped, aligning with the rise in viable cell density. While less reliable during high perfusion, cumulative oxygen input may be explored as an indirect indicator of cell growth. See Appendix D Figure D.2 for bioreactor run data.

The calculated accumulated antigen were approximately 299.5 kU for CA15-3, 497.0 kU for CA125 and 105.7 kU for CEA, indicating that CA125 was the dominant antigen produced. This pattern was also seen in the spinner cultures using CultiSpher G, although the ratio between CA15-3 and CA125 was slightly different. In the spinner culture, the ratio of CA15-3 to CA125 was approximately 1:4. In the bioreactor the ratio was closer to 3:5, showing a more balanced antigen production profile in the bioreactor.

Figure 4.11 shows CA15-3 productivity over time. During perfusion, momentary productivity peaked at about 18 kU/L/day. However, this is misleading. These values were calculated based on the antigen concentration and perfusion rate, since 0.5 L/day was removed, even low concentrations led to seemingly high values.

A more accurate productivity estimate uses the total harvested volume and average concentration (5.4 L at 37 U/mL), which equals 3.7 kU/L/day during perfusion. This is significantly lower than the peak productivity of 23 kU/L/day seen in the spinner culture using CultiSpher G.

Compared to the current roller production (8.6 kU/L/day), the bioreactor also underperformed. Despite the advantage of continuous nutrient renewal, low cell density during perfusion limited antigen yield.

Another important difference between the spinner flasks and bioreactor was the CO_2 environment. Spinner cultures were incubated in 8% CO_2, while the bioreactor had no CO_2 reference. This environmental difference might have affected cell growth, viability and productivity, especially for adherent cells like ZR75-1 that are sensitive to culture conditions. Additionally, fewer microcarriers were observed in the bioreactor samples compared to those from the spinner flasks. This could be due to microcarriers sticking to foam or the vessel walls, reducing the effective culture volume and available surface area for growth.

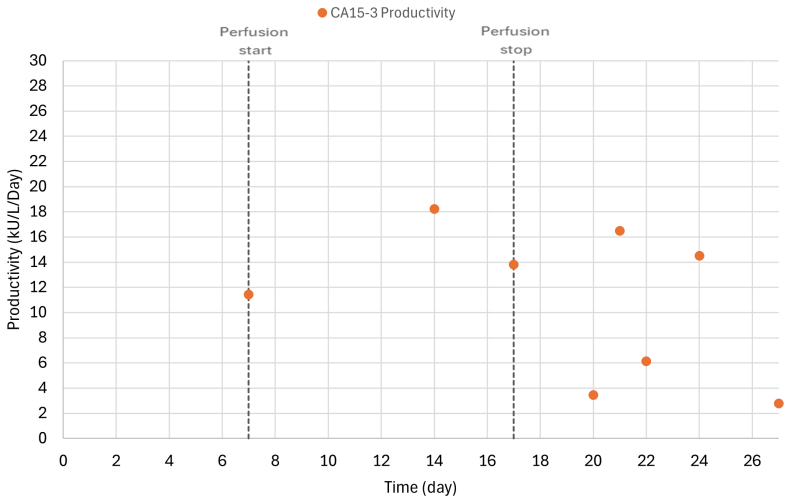

Figure 4.11. CA15-3 productivity in bioreactor culture 2 over time. Momentary values during perfusion (day 7–17) appear high, peaking at around 18 kU/L/day, but are misleading due to low antigen concentrations combined with a high perfusion rate (0.5 L/day). These values reflect calculated instantaneous productivity rather than actual yield.

These results show that while antigen levels eventually recovered after perfusion stopped, productivity and cell growth were lower than in spinner cultures. Several issues might have contributed, such as too early perfusion start, high shear stress and foam-induced carrier loss. However, bioreactor production still holds strong potential for CA15-3 manufacturing, provided that the process is further optimized to ensure stable culture conditions, efficient cell attachment and appropriate perfusion reference.

4.2.3 Bioreactor Culture 3

Bioreactor Culture 3 was conducted without perfusion and showed relatively low cell density throughout the 14-day culture period. Despite this, viability remained high during the entire culture, indicating that the conditions supported cell survival but not active proliferation. Data from the third bioreactor run is presented in Appendix D.

In this culture, unattached cells in the medium were measured to estimate attachment efficiency. The results, shown in Table 4.2, indicate a gradual increase in attachment over time, reaching 100% by day 8. This poor attachment, compared to the spinner flask attachment test, suggests that using a spinner step before bioreactor inoculation could help initiate adhesion under gentler conditions, possibly improving early cell distribution on microcarriers.

Table 4.2. Attachment percentage of ZR75-1 cells to CultiSpher® G microcarriers in Bioreactor Culture 3, calculated from unattached cell counts.

Day	Cells Attached (%)
1	52
4	75
6	75
8	100

4.3 Cellometer K2 is a Reliable Alternative to Manual Counting

One of the aims of this project was to identify a reliable method for counting ZR75-1 cells. To evaluate accuracy and consistency, 22 samples were analyzed using both a manual Bürker chamber and an automated Cellometer K2. Bürker counting was used as the reference method. The results are presented in Figure 4.12.

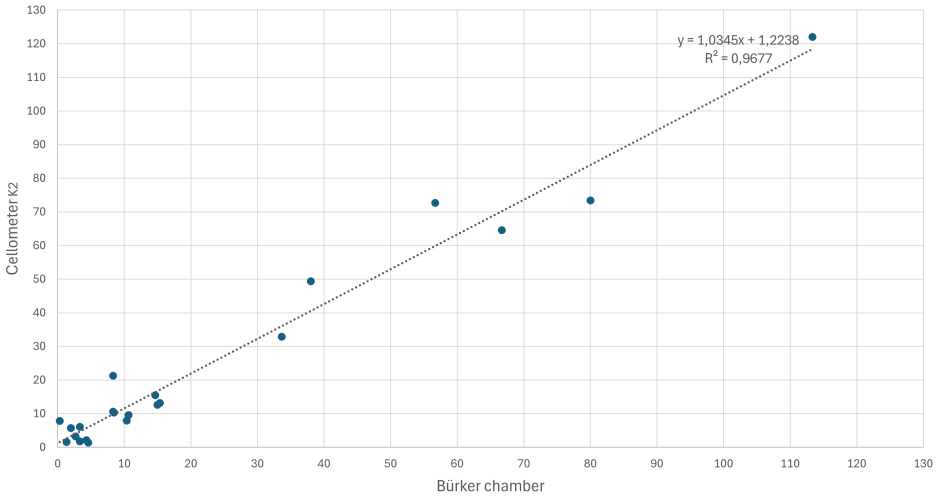

Figure 4.12. Comparison of cell density measurements using Bürker chamber and Cellometer K2 across 22 samples. $R^2 = 0.97$ and slope = 1.03. A paired two-tailed t-test showed no statistically significant difference between counting methods ($p = 0.12$).

The data shows a strong linear correlation between the two methods, with an R^2 value of 0.97 and a slope close to 1 (1.03), indicating good agreement. The y-intercept was low (1.22), but still shows that the Cellometer K2 generally gives a somewhat higher value.

To determine whether the two methods could be considered statistically equivalent, a paired two-tailed t-test was performed. The p-value was 0.12, which does not indicate a significant difference between the methods at a 95% confidence level ($p > 0.05$). Based on this, the Cellometer K2 results can be considered consistent with the Bürker chamber.

However, small deviations between the two methods were observed. These were in the same range or smaller than the variability typically seen when repeating counts on the same sample using the same method. This suggests that both approaches provide reproducible measurements and that the differences between them are within acceptable margins for practical use.

In summary, the Cellometer K2 provided comparable results to manual Bürker counting and can be used reliably for cell density estimation in this system.

4.4 Future Work

While this project demonstrates the feasibility of using microcarriers for ZR75-1 cell culture and CA15-3 production, several areas require further investigation to validate and optimize the proposed methods.

Although certain trends could be observed, additional replicates are needed to determine whether spinner and bioreactor cultivation of ZR75-1 cells does significantly improve antigen production and cell growth compared to when the cells are cultured in roller flasks.

Only a few microcarriers were tested in this project. Screening more types of microcarriers might identify better options for ZR75-1. Also, increasing the microcarrier concentration beyond 1 g/L should be tested, especially under perfusion, to support higher cell densities.

Future studies should evaluate the optimal inoculation method, including seeding density and stirring speed. Testing intermittent stirring during the attachment phase and different stirring speeds could improve early adhesion, minimizing the aggregation of free cells leading to increased microcarrier occupation.

The perfusion parameters used in this study was found to not be optimal. Future work should find the cell density required to start a successful perfusion. Also, evaluation of different perfusion rates for optimization should be done. Reducing shear stress in the tubing and cell separation system using gentler pumps may improve viability and productivity. Larger bioreactor volumes could also allow better reference over CSPR.

All cultures were performed in serum-containing medium. Transitioning to serum-free or defined media would reduce variability and improve process consistency. This would also decrease the foaming of medium which was a major problem. Medium optimization for ZR75-1 growth and CA15-3 production is a highly relevant area to further study.

Monitoring cell density in microcarrier cultures was done through sampling, which also removed microcarriers from the system. This can reduce available surface area over time, especially in small-volume bioreactors. Cell counting in these cultures is also challenging due to the difficulty of detaching cells from carriers. The Cellometer K2 showed good agreement with manual counting in this study but should be

further validated under higher-density conditions. Standardizing a reliable counting protocol will be important for future process reference. To minimize sampling and improve monitoring, alternative approaches such as online sensors should be explored. While oxygen consumption is commonly used to track metabolic activity, it did not reflect culture behavior well in the bioreactor runs performed in this study. Glucose levels could be a more sensitive indicator of metabolic activity and should be evaluated as a potential monitoring parameter in future studies.

5

Conclusion

The aim of this project was to explore the possibility of replacing the current roller bottle-based production of CA15-3 at FDAB with a more scalable and less labor-intensive method using microcarriers. Specifically, the goal was to evaluate different microcarriers to use with the adherent ZR75-1 cell line, scale up the method to a stirred-tank bioreactor with perfusion, and compare productivity with the already existing roller process.

From the microcarriers tested, CultiSpher G proved to be the most suitable for this purpose. It supported good growth of ZR75-1 cells over 28 days in spinner flask culture, with high cell viability maintained throughout. The productivity of CA15-3 reached a peak of around 23 kU/L/day in the spinner flask, well above the estimated 8.6 kU/L/day achieved in roller bottle production. This shows that the use of microcarriers can not only reduce the manual handling required in production but also increase antigen yield significantly.

The bioreactor cultures, however, showed more mixed results. While the microcarriers were successfully retained by the BioSep separation system, the cell density decreased once perfusion started. The productivity during perfusion, when calculated from the total harvest, was approximately 3.7 kU/L/day. This is lower than both the spinner culture and the roller production. Observations suggest that perfusion may have been started too early and that the culture was exposed to stress from foam formation, high CSPR, and shear forces in the tubing. These conditions likely limited both cell growth and antigen production.

The results from this project show that the microcarrier approach holds strong potential for producing CA15-3 with ZR75-1 cells. However, scaling up the process to bioreactor level requires further optimization. One key area is the attachment phase. Results from the attachment test showed that ZR75-1 cells attach slowly to CultiSpher G, and inefficient early attachment can lead to uneven microcarrier occupation and cell aggregation, which likely limits productivity. Sampling from bioreactor cultures also removes microcarriers and may further impact cell growth, pointing to the need for better monitoring tools or reduced sampling frequency.

Some limitations of this study include the number of replicates, which may affect the reliability of the results. Additionally, the relatively short run time of some cultures due to infection impacted the overall duration of the experiment. Another

challenge was comparing cell growth across different microcarriers, as cell counting proved difficult.

To verify these results and move toward implementation, further studies should focus on optimizing inoculation and attachment conditions, including testing intermittent stirring and different seed densities. It would also be valuable to test higher microcarrier concentrations and lower perfusion rates, possibly using larger bioreactor volumes to reduce relative media exchange. Investigating serum-free media and better defining how culture conditions affect antigen composition and downstream processing will also be important.

In summary, this project shows that microcarrier-based cultures using CultiSpher G can increase CA15-3 productivity and support long-term cell growth with ZR75-1 cells. While the bioreactor culture needs more work, the results are promising and show that this approach has clear potential to improve and automatize the antigen production process at FDAB.

Bibliography

[1] A. L. Van Wezel, "Growth of Cell-strains and Primary Cells on Micro-carriers in Homogeneous Culture," *Nature 1967 216:5110*, vol. 216, no. 5110, pp. 64–65, 1967. [Online]. Available: https://www.nature.com/articles/216064a0

[2] X. Y. Chen, J. Y. Chen, X. M. Tong, J. G. Mei, Y. F. Chen, and X. Z. Mou, "Recent advances in the use of microcarriers for cell cultures and their ex vivo and in vivo applications," *Biotechnology Letters*, vol. 42, no. 1, pp. 1–10, 1 2020. [Online]. Available: https://link.springer.com/article/10.1007/s10529-019-02738-7

[3] Cytiva, "Principles and methods," 2021. [Online]. Available: https://cdn.cytivalifesciences.com/api/public/content/digi-11250-pdf?_gl=1*1vmbo63*_gcl_au*OTk4NDcxMjAyLjE3Mzc1Mzg3Nzg.*_ga*MTQ5ODcxNDU3Ni4xNzM3NTM4ODAz*_ga_CS9H0CZBWW*MTczNzcwNjY0OS4yLjAuMTczNzcwNjY0OS4wLjAuMA..

[4] K. Wilson and J. Walker, *Principles and Techniques of Biochemistry and Molecular Biology*, K. Wilson and J. Walker, Eds. Cambridge University Press, 3 2005.

[5] F. M. Lydyard Peter, Whelan Alex, *Immunology* , 3rd ed. New York: Taylor & Francis Group, 2011.

[6] J. Charles A Janeway, P. Travers, M. Walport, and M. J. Shlomchik, "Immunobiology," *Immunobiology*, no. 14102, pp. 1–10, 2001. [Online]. Available: https://www.ncbi.nlm.nih.gov/books/NBK10757/

[7] Y. Zhou, L. Tao, J. Qiu, J. Xu, X. Yang, Y. Zhang, X. Tian, X. Guan, X. Cen, and Y. Zhao, "Tumor biomarkers for diagnosis, prognosis and targeted therapy," *Signal Transduction and Targeted Therapy 2024 9:1*, vol. 9, no. 1, pp. 1–86, 5 2024. [Online]. Available: https://www.nature.com/articles/s41392-024-01823-2

[8] N. C. Japp, J. J. Souchek, A. R. Sasson, M. A. Hollingsworth, S. K. Batra, and W. M. Junker, "Tumor Biomarker In-Solution Quantification, Standard Production, and Multiplex Detection," *Journal of Immunology Research*, vol. 2021, no. 1, p. 9942605, 1 2021. [Online]. Available: https://onlinelibrary.wiley.com/doi/full/10.1155/2021/9942605https:

//onlinelibrary.wiley.com/doi/abs/10.1155/2021/9942605https://onlinelibrary.wiley.com/doi/10.1155/2021/9942605

[9] "Tumor Markers - NCI." [Online]. Available: https://www.cancer.gov/about-cancer/diagnosis-staging/diagnosis/tumor-markers-fact-sheet

[10] F. Naghibalhossaini and P. Ebadi, "Evidence for CEA release from human colon cancer cells by an endogenous GPI-PLD enzyme," *Cancer Letters*, vol. 234, no. 2, pp. 158–167, 3 2006. [Online]. Available: https://www.sciencedirect.com/science/article/pii/S030438350500279X

[11] B. L. Witt and T. O. Tollefsbol, "Molecular, Cellular, and Technical Aspects of Breast Cancer Cell Lines as a Foundational Tool in Cancer Research," *Life 2023, Vol. 13, Page 2311*, vol. 13, no. 12, p. 2311, 12 2023. [Online]. Available: https://www.mdpi.com/2075-1729/13/12/2311/htmhttps://www.mdpi.com/2075-1729/13/12/2311

[12] . L. W. E. Pathology, M. J. J. Â¡, and M. Branch, "Establishment and Characterization of Three New Continuous Cell Lines Derived from Human Breast Carcinomas and Laboratory of Viral Carcinogenes/s Â¡S." [Online]. Available: http://aacrjournals.org/cancerres/article-pdf/38/10/3352/2401107/cr0380103352.pdf

[13] Y. Fu and H. Li, "Assessing Clinical Significance of Serum CA15-3 and Carcinoembryonic Antigen (CEA) Levels in Breast Cancer Patients: A Meta-Analysis," *Medical Science Monitor : International Medical Journal of Experimental and Clinical Research*, vol. 22, p. 3154, 9 2016. [Online]. Available: https://pmc.ncbi.nlm.nih.gov/articles/PMC5022658/

[14] W. Chen, Z. Zhang, S. Zhang, P. Zhu, J. K. S. Ko, and K. K. L. Yung, "MUC1: Structure, Function, and Clinic Application in Epithelial Cancers," *International Journal of Molecular Sciences*, vol. 22, no. 12, p. 6567, 6 2021. [Online]. Available: https://pmc.ncbi.nlm.nih.gov/articles/PMC8234110/

[15] M. J. Duffy, D. Evoy, and E. W. McDermott, "CA 15-3: Uses and limitation as a biomarker for breast cancer," *Clinica Chimica Acta*, vol. 411, no. 23-24, pp. 1869–1874, 12 2010. [Online]. Available: https://www.sciencedirect.com/science/article/pii/S0009898110005589

[16] Fujirebio Diagnostics AB, "CanAg CA15-3 EIA," Mölndal, 5 2023. [Online]. Available: https://www.fujirebio.com/en/products-solutions/canag-ca153-eia

[17] G. L. PERKINS, E. D. SLATER, G. K. SANDERS, and J. G. PRICHARD, "Serum Tumor Markers," *American Family Physician*, vol. 68, no. 6, pp. 1075–1082, 9 2003. [Online]. Available: https://www.aafp.org/pubs/afp/issues/2003/0915/p1075.html

[18] V. L. Kankanala, M. Zubair, and S. K. R. Mukkamalla, "Carcinoembryonic Antigen," *StatPearls*, 12 2024. [On-

line]. Available: https://www.ncbi.nlm.nih.gov/books/NBK578172/http://www.pubmedcentral.nih.gov/articlerender.fcgi?artid=PMC5482067

[19] Fujirebio Diagnostics AB, "CanAg CEA EIA," Mölndal, 5 2023. [Online]. Available: https://www.fujirebio.com/en/products-solutions/canag-cea-eia

[20] C. Whitehouse and E. Solomon, "Current Status of the Molecular Characterization of the Ovarian Cancer Antigen CA125 and Implications for Its Use in Clinical Screening," *Gynecologic Oncology*, vol. 88, no. 1, pp. S152–S157, 1 2003.

[21] P. Charkhchi, C. Cybulski, J. Gronwald, F. O. Wong, S. A. Narod, and M. R. Akbari, "CA125 and Ovarian Cancer: A Comprehensive Review," *Cancers*, vol. 12, no. 12, p. 3730, 12 2020. [Online]. Available: https://pmc.ncbi.nlm.nih.gov/articles/PMC7763876/

[22] K. Hande and T. Butler, "Cancer Antigen 125," *Laboratory Screening and Diagnostic Evaluation: An Evidence-Based Approach*, pp. 173–177, 5 2024. [Online]. Available: https://www.ncbi.nlm.nih.gov/books/NBK562245/

[23] Fujirebio Diagnostics AB, "CanAg CA125 EIA," Mölndal, 5 2023. [Online]. Available: https://www.fujirebio.com/en/products-solutions/canag-ca125-eia

[24] S. Derakhti, S. H. Safiabadi-Tali, G. Amoabediny, and M. Sheikhpour, "Attachment and detachment strategies in microcarrier-based cell culture technology: A comprehensive review," *Materials Science and Engineering: C*, vol. 103, p. 109782, 10 2019.

[25] M. M. Zhu, M. Mollet, R. S. Hubert, Y. S. Kyung, and G. G. Zhang, "Industrial Production of Therapeutic Proteins: Cell Lines, Cell Culture, and Purification."

[26] K. Kendall, M. Kendall, and F. Rehfeldt, "Adhesion of Cells," *Adhesion of Cells, Viruses and Nanoparticles*, pp. 221–240, 2010. [Online]. Available: https://link.springer.com/chapter/10.1007/978-90-481-2585-2_10

[27] A. A. Khalili and M. R. Ahmad, "A Review of Cell Adhesion Studies for Biomedical and Biological Applications," *International Journal of Molecular Sciences*, vol. 16, no. 8, p. 18149, 8 2015. [Online]. Available: https://pmc.ncbi.nlm.nih.gov/articles/PMC4581240/

[28] X. Zhang, Y. Wen, and S. T. Yang, "Modes of Culture/Animal Cells," *Comprehensive Biotechnology, Second Edition*, vol. 1, pp. 285–302, 1 2011.

[29] C. F. Bellani, J. Ajeian, L. Duffy, M. Miotto, L. Groenewegen, and C. J. Connon, "Scale-Up Technologies for the Manufacture of Adherent Cells," *Frontiers in Nutrition*, vol. 7, p. 575146, 11 2020. [Online]. Available: www.frontiersin.org

[30] S. Ozturk and W. S. Hu, "Cell Culture Technology for Pharmaceutical and Cell-Based Therapies," *Cell Culture Technology for Pharmaceutical and Cell-Based Therapies*, pp. 1–769, 1 2005.

[31] V. Noel and M. D. Berry, "Culture of Adherent Cancer Cell Lines," *Methods in Molecular Biology*, vol. 2508, pp. 19–29, 2022. [Online]. Available: https://link.springer.com/protocol/10.1007/978-1-0716-2376-3_3

[32] M. Taya and M. Kino-oka, "Bioreactors for Animal Cell Cultures," *Comprehensive Biotechnology, Second Edition*, vol. 2, pp. 373–382, 1 2011.

[33] F. Garcia-Ochoa, V. E. Santos, and E. Gomez, "Stirred Tank Bioreactors," *Comprehensive Biotechnology, Second Edition*, vol. 2, pp. 179–198, 1 2011.

[34] S. S. Ozturk, "Engineering challenges in high density cell culture systems," *Cytotechnology*, vol. 22, no. 1-3, pp. 3–16, 1996. [Online]. Available: https://link.springer.com/article/10.1007/BF00353919

[35] X. Liu and P. Raju, "In Vitro Cancer Model for Drug Testing," *Comprehensive Biotechnology, Second Edition*, vol. 5, pp. 543–549, 1 2011.

[36] J. M. Bielser, M. Wolf, J. Souquet, H. Broly, and M. Morbidelli, "Perfusion mammalian cell culture for recombinant protein manufacturing – A critical review," *Biotechnology Advances*, vol. 36, no. 4, pp. 1328–1340, 7 2018.

[37] M. J. Rice and D. Miller, "Principles of Mammalian Cell Culture Process Scale-up."

[38] S. F. Gorfien, A. Campbell, and M. C. Vemuri, "Design of Culture Media," *Comprehensive Biotechnology, Second Edition*, vol. 1, pp. 205–215, 1 2011.

[39] Sigma Aldrich, "Dulbecco's Modified Eagle Medium (DMEM)." [Online]. Available: https://www.sigmaaldrich.com/SE/en/products/cell-culture-and-analysis/cell-culture-media-and-buffers/classical-media-and-buffers/dulbeccos-modified-eagle-medium

[40] J. van der Valk, K. Bieback, C. Buta, B. Cochrane, W. G. Dirks, J. Fu, J. J. Hickman, C. Hohensee, R. Kolar, M. Liebsch, F. Pistollato, M. Schulz, D. Thieme, T. Weber, J. Wiest, S. Winkler, and G. Gstraunthaler, "Fetal Bovine Serum (FBS): Past - Present - Future," *ALTEX*, vol. 35, no. 1, pp. 99–118, 2018. [Online]. Available: https://pubmed.ncbi.nlm.nih.gov/28800376/

[41] C. E. Jochems, J. B. Van der Valk, F. R. Stafleu, and V. Baumans, "The use of fetal bovine serum: Ethical or scientific problem?" *Alternatives to Laboratory Animals*, vol. 30, no. 2, pp. 219–227, 2002.

[42] M. Baker, "Reproducibility: Respect your cells!" *Nature 2016 537:7620*, vol. 537, no. 7620, pp. 433–435, 9 2016. [Online]. Available: https://www.nature.com/articles/537433a

[43] S. Mukherjee, P. Malik, and T. K. Mukherjee, "Mammalian Cell Culture: An Overview," *Practical Approach to Mammalian Cell and Organ Culture: With 261 Figures and 89 Tables*, pp. 1–41, 1 2022. [Online]. Available: https://link.springer.com/referenceworkentry/10.1007/978-981-19-1731-8_1-1

[44] B. Li, X. Wang, Y. Wang, W. Gou, X. Yuan, J. Peng, Q. Guo, and S. Lu, "Past, present, and future of microcarrier-based tissue engineering," *Journal of Orthopaedic Translation*, vol. 3, no. 2, p. 51, 4 2015. [Online]. Available: https://pmc.ncbi.nlm.nih.gov/articles/PMC5982391/

[45] "FAQ | Percell Biolytica." [Online]. Available: https://percell.se/faq/#toggle-id-5-closed

[46] K. W. Wissemann and B. S. Jacobson, "Pure gelatin microcarriers: Synthesis and use in cell attachment and growth of fibroblast and endothelial cells," *In Vitro Cellular & Developmental Biology*, vol. 21, no. 7, pp. 391–401, 7 1985. [Online]. Available: https://link.springer.com/article/10.1007/BF02623470

[47] "BioNOC II® Cell Culture Macrocarriers | Esco Healthcare." [Online]. Available: https://escovaccixcell.com/tide_technology/cell_attachment/BioNOC_II

[48] "Fibra-Cel® Disks." [Online]. Available: https://www.eppendorf.com/gb-en/Products/Bioprocess/Bioprocess-Accessories/Fibra-Cel-Disks-p-PF-67052

[49] S. P. Forestell, N. Kalogerakis, L. A. Behie, and D. F. Gerson, "Development of the optimal inoculation conditions for microcarrier cultures," *Biotechnology and Bioengineering*, vol. 39, no. 3, pp. 305–313, 1992.

[50] T. J. Nikolai and W. S. Hu, "Cultivation of mammalian cells on macroporous microcarriers," *Enzyme and microbial technology*, vol. 14, no. 3, pp. 203–208, 1992. [Online]. Available: https://pubmed.ncbi.nlm.nih.gov/1372509/

[51] "HYCLONE MEDIA AND SUPPLEMENTS CultiSpher gelatine microcarriers," 2020.

[52] J. Scibek and Z. Melkoumian, "Corning ® Enhanced Attachment Microcarriers Show Improved Expansion of Vero Cells for Bioprocess Applications Compared to Competitor Application Note." [Online]. Available: www.corning.com/lifesciences.

[53] K. Nilsson, "Microcarrier Cell Culture," *Biotechnology and Genetic Engineering Reviews*, vol. 6, no. 1, pp. 404–439, 1988. [Online]. Available: https://www.tandfonline.com/action/journalInformation?journalCode=tbgr20

[54] P. Dosta, S. Ferber, Y. Zhang, K. Wang, A. Ros, N. Uth, Y. Levinson, E. Abraham, and N. Artzi, "Scale-up manufacturing of gelatin-based microcarriers for cell therapy," *Journal of Biomedical Materials Research - Part B Applied Biomaterials*, vol. 108, no. 7, pp. 2937–2949, 10 2020.

[55] K. E. Strathearn, A. Maria, and P. Pardo, "Parameters to Consider When Expanding Cells on Corning ® Microcarriers Application Note."

[56] Q. A. Rafiq, K. Coopman, A. W. Nienow, and C. J. Hewitt, "Systematic microcarrier screening and agitated culture conditions improves

human mesenchymal stem cell yield in bioreactors," *Biotechnology Journal*, vol. 11, no. 4, pp. 473–486, 4 2016. [Online]. Available: https://onlinelibrary.wiley.com/doi/full/10.1002/biot.201400862https://onlinelibrary.wiley.com/doi/abs/10.1002/biot.201400862https://analyticalsciencejournals.onlinelibrary.wiley.com/doi/10.1002/biot.201400862

[57] Q. A. Rafiq, K. M. Brosnan, K. Coopman, A. W. Nienow, and C. J. Hewitt, "Culture of human mesenchymal stem cells on microcarriers in a 5 l stirred-tank bioreactor," *Biotechnology Letters*, vol. 35, no. 8, pp. 1233–1245, 8 2013. [Online]. Available: https://link.springer.com/article/10.1007/s10529-013-1211-9

[58] David Runquist and Karin Nilsson, "TEST AV MICORCARRIERS FÖR ODLING AV ADHERENTA CELLINJER," Gothenburg, 2011.

[59] ——, "ZR75-1 Bioreactor Microcarrier "Proof of Principle 2"," Gothenburg, 2011.

[60] Karin Nilsson and Lina Lövgren, "Bioreaktorodling 1," Gothenburg, 2015.

[61] ——, "Bioreaktorodling 2," Gothenburg, 2015.

[62] Lina Lövgren, "Microcarrierförsök ," Gothenburg, 2015.

[63] J. M. Van Emon, "Immunoassays in Biotechnology," *Comprehensive Biotechnology, Second Edition*, vol. 1, pp. 659–667, 1 2011.

[64] A. Hofmann and S. Clokie, *Wilson and Walker's Principles and Techniques of Biochemistry and Molecular Biology*. Cambridge University Press, 2018.

[65] R. P. Vynohradova, "Units of enzyme activity," *Ukrainskii biokhimicheskii zhurnal*, vol. 71, no. 2, pp. 96–99, 1999.

[66] "This protocol is meant as a starting point for user optimization of microcarrier culture, specifically for use with Corning Microcarriers," 2013. [Online]. Available: www.corning.com/lifesciences/trademarks.

[67] C. Sion, C. Loubière, M. K. Wlodarczyk-Biegun, N. Davoudi, C. Müller-Renno, E. Guedon, I. Chevalot, and E. Olmos, "Effects of microcarriers addition and mixing on WJ-MSC culture in bioreactors," *Biochemical Engineering Journal*, vol. 157, p. 107521, 4 2020.

[68] J.-T. Gatan, "Percell Biolytica AB."

[69] A. Werner, S. Duvar, J. Müthing, H. Büntemeyer, H. Lünsdorf, M. Strauss, and J. Lehmann, "Cultivation of immortalized human hepatocytes HepZ on macroporous CultiSpher G microcarriers," *Biotechnology and Bioengineering*, vol. 68, no. 1, pp. 59–70, 4 2000.

A

Enzymatic Immunoassays

Protocols followed for the EIAs used are presented below. The protocols were obtained from the immunoassay kits produced by FDAB [**?**, 16, 23]

A.1 CanAg CA15-3 Enzyme Immunoassay

The desired amount of strips, depending on the sample size, was taken from a streptavidin coated microplate with breakable cells. The strips were placed in a frame and each well was washed once with prepared wash buffer in a HydroFlex™ Plus microplate washer (TECAN). Antibody solution was prepared according to the number of strips. For example, three strips 150 ml tracer (Horseradish peroxidase labelled with CA15-3 MAb) were mixed with 3 ml biotin in a 15 ml tube. 25 µl of each sample was mixed with 1 ml of sample diluent. Calibrators with CA15-3 concentration 0, 15, 50, 125 and 250 U/ml were added to the microplate in duplicates, 25 µl in each well. The samples were added in the same way and 100 µl antibody solution (Biotin Anti-CA15-3 MAb) was added to all wells. The plate was then incubated for 2 hours shaking at room temperature. Then, each well was washed 6 times and 100 µl substrate (3,3',5,5' tetramethyl-benzidine) was added. The microplate was incubated for 30 min shaking at room temperature and then the absorbance was read at 620 nm with a ELx808^{TM} Absorbance Microplate Reader (BioTek).

A.2 CanAg CA125 Enzyme Immunoassay

The desired amount of strips, depending on the sample size, was taken from a streptavidin coated microplate with breakable cells. The strips were placed in a frame and each well was washed once with prepared wash buffer in a HydroFlex™ Plus microplate washer (TECAN) in plate mode. Tracer working solution was prepared according to the number of strips. For example, for three strips, 150 ml tracer (Horseradish peroxide labelled with CA125 MAb) was mixed with 3 ml Tracer Diluent in a 15 ml tube. Calibrators with CA125 concentration 0, 10, 40, 200 and 500 U/ml were added to the microplate in duplicates, 25 µl in each well. The samples were added in the same way and 100 µl Biotin Anti-CA125 MAb was added to all wells. The plate was then incubated for 2 hours shaking at room temperature. Each well was then washed 3 times with wash solution in plate mode and 100 µl Tracer

working solution was added to each well. The microplate was then incubated for 1 hour shaking at room temperature. Then the plate was washed 6 times in plate mode and 100 µl of TMB was added to each well. The plate was incubated for 30 min shaking at room temperature. The absorbance was read at 620 nm with a ELx808^{TM} Absorbance Microplate Reader (BioTek). Results were multiplied by 1.23, a standard procedure at FDAB.

A.3 CanAg CEA Enzyme Immunoassay

The desired amount of strips, depending on the sample size, was taken from a streptavidin coated microplate with breakable cells. The strips were placed in a frame and each well was washed once with prepared wash buffer in a HydroFlex™ Plus microplate washer (TECAN). Antibody solution was prepared according to the number of strips. For example, three strips 150 ml tracer (Horseradish peroxidase labelled with CEA MAb) were mixed with 3 ml biotin in a 15 ml tube. 25 µl of each sample was mixed with 1 ml of sample diluent. Calibrators with CA14-3 concentration 0, 2, 5, 15, 50 and 75 U/ml were added to the microplate in duplicates, 25 µl in each well. The samples were added in the same way and 100 µl antibody solution (Biotin Anti-CEA MAb) was added to all wells. The plate was then incubated for 1 hour shaking at room temperature. Then, each well was washed 6 times and 100 µl TMB was added. The microplate was incubated for 30 min shaking at room temperature and then the absorbance was read at 620 nm with a ELx808^{TM} Absorbance Microplate Reader (BioTek).

B

Spinner Culture Data

Data for measured cell density, viability and antigen concentration in the spinner flask are presented below.

B.1 Concentration Measurements in Spinner Round 3

The EIA-measured antigen concentrations for all spinners in round 3 are presented in Table B.1. The presented values are the mean of two replicates.

Table B.1. Antigen concentrations (CA15-3, CA125, CEA) in the three spinner cultures over time.

Date	Day	CultiSpher G (U/mL)			Fibra-Cel Disk (U/mL)			Reference (U/mL)		
		CA15-3	CA125	CEA	CA15-3	CA125	CEA	CA15-3	CA125	CEA
250428	5	40.54	66.62	4.31	33.64	22.73	3.33	44.31	50.56	6.00
250502	9	50.03	130.61	9.88	29.97	13.32	3.00	51.76	64.19	11.10
250506	13	77.25	217.55	22.11	55.20	18.10	5.75	72.71	118.26	23.31
250509	16	97.45	270.84	27.55	42.61	15.64	4.51	75.51	129.92	29.09
250513	20	141.40	416.96	50.22	-	-	-	105.59	189.43	53.35
250516	23	121.80	481.95	62.78	-	-	-	99.44	187.75	56.89
250519	26	129.54	615.00	78.75	-	-	-	103.13	203.17	67.57
252521	28	101.03	595.08	78.75	-	-	-	83.54	163.66	49.94

B.2 Cell Density and Viability Measured in Cultispher G Spinner

The cell density and viability measured in Cultispher G spinner, round 3, is presented in Table B.2. The cell density presented is a mean of the values from the Bürker chamber and Cellometer K2.

B.2.1 CA15-3 Concentration Comparison of Spinner Round 3

The measured concentrations of antigen from the three different spinners in round 3 by EIA is presented in Table B.3. Table B.4 presents the comparison of the con-

Table B.2. Viable cell density and viability of CultiSpher G Spinner flask, round 3.

Date	**Day**	**Viable Cell Density** ($\times 10^4$ cells/mL)
250423	0	15.05
250428	5	4.07
250502	9	14.82
250506	13	33.28
250509	16	117.67
250513	20	76.70
250516	23	43.70
250519	26	64.685
252521	28	65.635

centration in each time point by Student's t-test. The threshold p-value is $p<0.05$.

Table B.3. CA15-3 concentrations (μU/mL) in spinner cultures with different microcarriers. Each condition was measured in duplicates.

Day	**Replicate**	**CultiSpher G**	**None**	**Fibra-Cel Disk**
5	1	40.207	45.350	34.288
	2	40.868	43.271	32.981
9	1	50.537	53.570	30.049
	2	49.537	49.949	29.887
13	1	77.290	73.021	55.877
	2	77.211	72.392	54.514
16	1	99.191	76.665	43.381
	2	95.698	74.361	41.832
20	1	143.856	103.724	–
	2	138.946	107.454	–
23	1	124.842	100.278	–
	2	118.759	98.607	–
26	1	126.890	103.302	–
	2	132.193	102.965	–
28	1	100.110	86.601	–
	2	101.955	80.479	–

Table B.4. P-values from Student's t-test comparing CA15-3 concentrations between conditions at each time point. Significant differences ($p < 0.05$) are highlighted.

Day	CultiSpher vs None	CultiSpher vs Fibra-Cel	None vs Fibra-Cel
5	0.074	**0.011**	**0.013**
9	0.456	**0.001**	**0.007**
13	**0.005**	**0.001**	**0.002**
16	**0.009**	**0.001**	**0.002**
20	**0.007**	–	–
23	**0.019**	–	–
26	**0.010**	–	–
28	**0.032**	–	–

C

Cell Attachment Measurements

The data of the cell attachment test is presented in Table C.1. It shows the measured cell densities in the culture medium, representing the unattached cells. Cell densities were measured in a Bürker chamber.

Table C.1. Cell density of unattached cells in medium (CultiSpher G, Spinner 3).

Time (h)	**Cell Density** ($\times 10^4$ cells/mL)
0	29.3
1	29.1
2	29.3
3	18.2
4	18.2
5	17.9
6	13.2
7	9.24
8	10.3
23	3.33

D

Bioreactor Data

This Appendix presents the data obtained from the bioreactor cultures.

D.1 Bioreactor Inoculation 1

Figure D.1 presents the Livit Flex output from inoculation 1, including the air, oxygen, temperature and DO.

D.2 Bioreactor Inoculation 2

Figure D.2 presents the Livit Flex output from inoculation 1, including the air, oxygen, temperature and DO. In Table D.1 the viable cell density and measured antigen concentrations of CA15-3, CEA and CA125 are presented.

Table D.1. Viable cell density and measured antigen concentrations for bioreactor culture 2.

Date	**Day**	**Viable cell density** (x10^4 cells/mL)	**CA15-3** (U/mL)	**CA125** (U/mL)	**CEA** (U/mL)
250408	0	9.118	0.000	0.000	0.000
250415	7	14.265	80.097	64.919	6.781
250422	14	9.370	36.707	55.699	10.451
250425	17	3.215	25.397	51.619	9.633
250428	20	3.010	35.722	75.532	18.079
250429	21	10.120	52.229	84.671	20.248
250430	22	9.467	58.362	98.750	25.156
250502	24	3.850	87.386	121.813	36.700
250505	27	1.465	95.745	161.894	51.477

D.3 Bioreactor Inoculation 3

Figure D.3 presents the Livit Flex output from inoculation 1, including the air, oxygen, temperature and DO. In Table D.2 the viable cell density and measured antigen

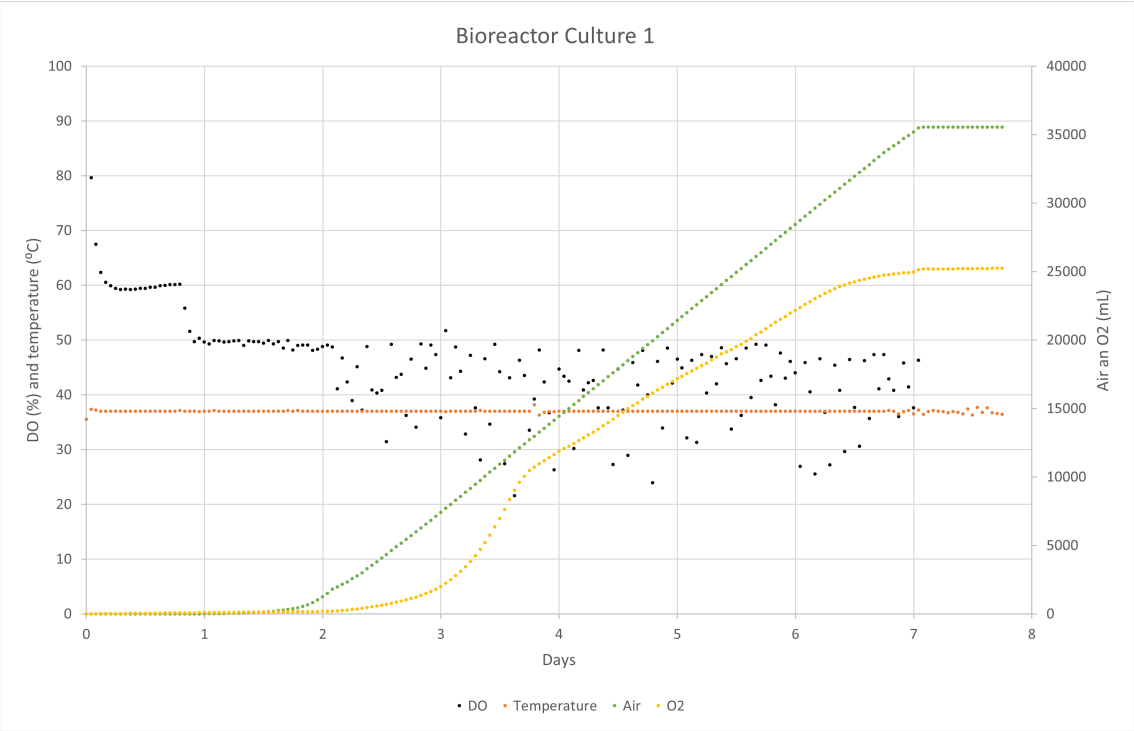

Figure D.1. Online data from Bioreactor Culture 1 showing dissolved oxygen (DO), temperature, and total sparged air and oxygen volumes over time. A steady increase in gas flow was required to maintain DO setpoint during the batch culture.

concentrations of CA15-3, CEA and CA125 are presented. This data is visualised in Figure D.4 showing the cell density, viability and calculated productivity.

Table D.2. Bioreactor Culture 3: Cell density distribution, viability, and antigen concentrations over time.

Day	**Cells in medium** ($\times 10^4$ cells/mL)	**Cells on carriers** ($\times 10^4$ cells/mL)	**Total density** ($\times 10^4$ cells/mL)	**Viab.**	**CA15-3** (U/mL)	**CA125** (U/mL)	**CEA** (U/mL)
0	7.8	0.00	7.8	95%			
1	4.33	4.67	9.0	75	10.55	5.93	0.61
4	0.33	1.00	1.33	100%	17.83	7.40	1.31
6	1.00	3.00	4.0	100%	25.90	13.58	3.27
8	0.00	3.33	3.33	100%	31.34	18.40	5.92
11	0.00	2.67	2.67	100%	46.23	28.36	10.27
13	0.00	4.68	4.68	95%	51.65	35.29	11.77

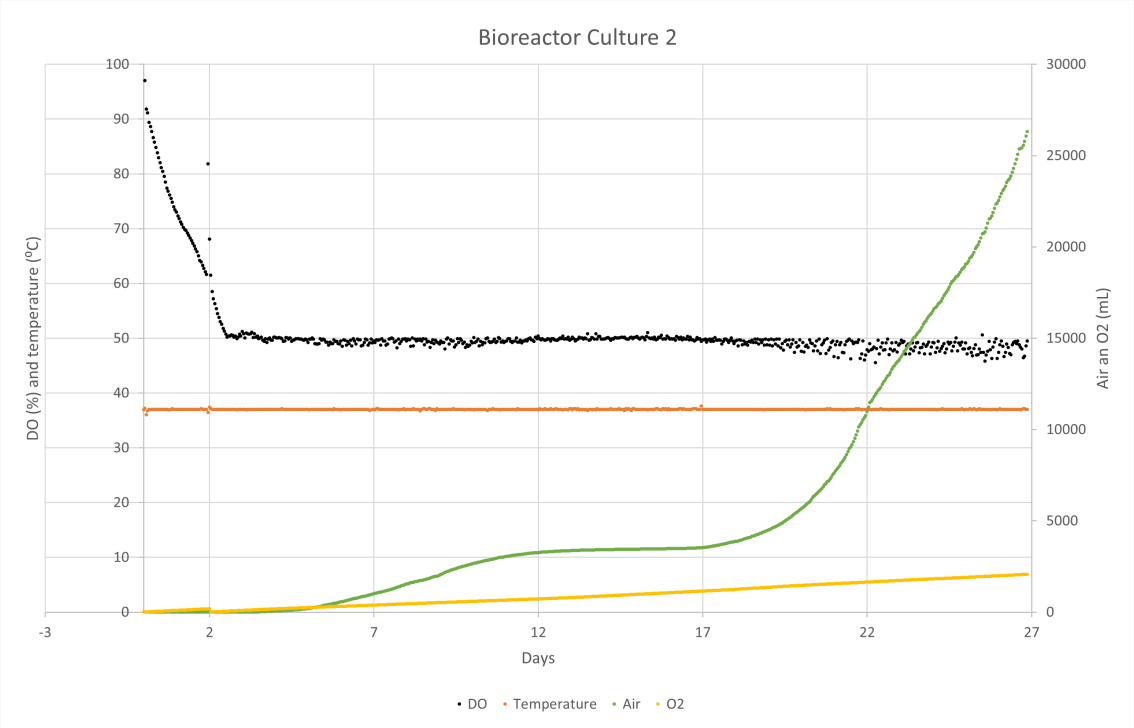

Figure D.2. Online control data from Bioreactor Culture 2 including DO, temperature, and total sparged air and oxygen volumes. Perfusion ran from day 7 to 17. Increasing oxygen addition correlated with rising cell density until perfusion stopped.

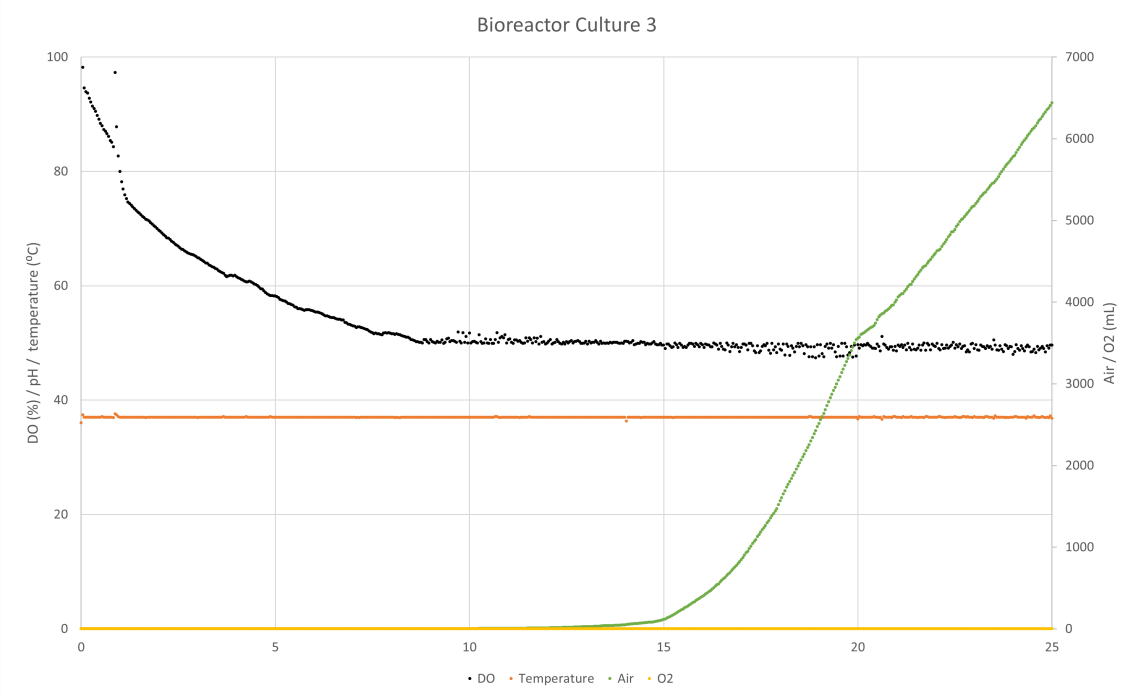

Figure D.3. Online control data from Bioreactor Culture 3 including DO, temperature, and total sparged air and oxygen volumes. Fed-batch culture.

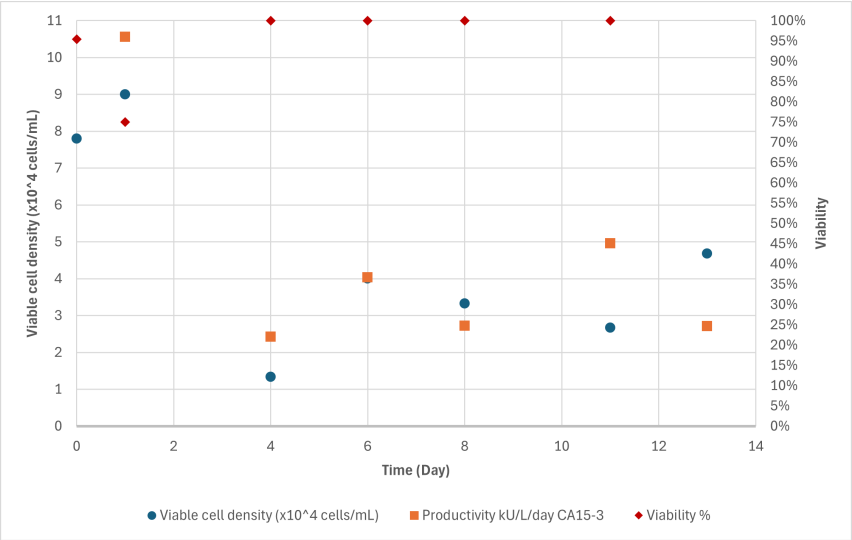

Figure D.4. Cell density, vibility and calculated productivity of biorector inoculation 3.

E

Cell-Specific Perfusion Rate Calculation

This Appendix presents the calculated Cell-Specific Perfusion Rate (CSPR) for both spinner and bioreactor cultures. For spinner flasks, CSPR was estimated from medium exchange volumes and intervals according to Equation E.1.

$$\text{Perfusion Rate} = \frac{V_{replaced}}{\Delta t} \tag{E.1}$$

$V_{replaced}$ is the volume (ml) replaced at each occasion and Δt is the number of days since the last medium replacement.

For the bioreactor, values were calculated based on continuous perfusion rates and measured cell densities based on equation 2.2 in the Theory section.

The corresponding perfusion rates and CSPR values are shown in Table E.1.

Table E.1. Calculated Cell-Specific Perfusion Rate (CSPR) for spinner and bioreactor cultures with corresponding perfusion rates.

Day	**Perf. rate spinner (L/day)**	**CSPR Spinner (pL/cell/day)**	**Perf. rate bioreactor (L/day)**	**CSPR Bioreactor (pL/cell/day)**
5	0.06	1327.43	–	–
7	0.0375	–	0.50	5336.18
9	0.0375	3073.77	–	–
13	0.05	842.70	–	–
14	0.0375	–	0.54	16770.19
16	0.05	500.50	–	–
20	0.05	106.23	–	–
23	0.075	217.30	–	–
26	–	381.39	–	–
28	–	386.40	–	–

F

Scale Up Calculations

To estimate suitable agitation parameters for scaling up from spinner flask to bioreactor, tip speed were calculated. Table F.1 presents the parameters from the spinner flask system, and Table F.2 shows the corresponding calculated values for the 3 L bioreactor using equivalent tip speeds.

Table F.1. Parameters for spinner culture used in bioreactor upscaling calculations.

Parameter	**Value**	**Unit**
Reactor volume (V)	0.5	L
Impeller diameter (d_s)	0.075	m
Density (ρ)	1000	kg/m^3
Viscosity (μ)	0.000089	kg/ms
Minimum RPM (n_{rpm})	30	1/min
Maximum RPM (n_{rpm})	40	1/min
Minimum RPS (n_{rps})	0.5	1/s
Reynolds number (min)	31601	-
Tip speed (min) (v_{tip})	0.12	m/s
Maximum RPS (n_{rps})	0.7	1/s
Reynolds number (max)	42135	-
Tip speed (max) (v_{tip})	0.16	m/s

Table F.2. Calculated equivalent parameters for 3 L bioreactor based on spinner culture tip speed.

Parameter	**Value**	**Unit**
Reactor volume (V)	3.0	L
Impeller diameter (d_s)	0.03	m
Density (ρ)	1010	kg/m^3
Viscosity (μ)	0.000089	kg/ms
Tip speed (min) (v_{tip})	0.12	m/s
Minimum RPS (n_{rps})	1.3	1/s
Minimum RPM (n_{rpm})	75	1/min
Reynolds number (min)	12767	-
Tip speed (max) (v_{tip})	0.16	m/s
Maximum RPS (n_{rps})	1.7	1/s
Maximum RPM (n_{rpm})	100	1/min
Reynolds number (max)	17022	-

G

Counting Method Comparison Data

This Appendix present the data used for the comparison of Bürker chamber and Cellometer K2.

Table G.1. Comparison of cell concentrations measured using Bürker chamber and Cellometer K2 for 22 samples. Values are given in $\times 10^4$ cells/mL.

Sample	Bürker	Cellometer
1	10.36	7.875
2	15.33	13.2
3	8.44	10.3
4	4.3	2.13
5	4.6	1.42
6	10.66	9.58
7	8.33	10.6
8	2.00	5.7
9	1.33	1.6
10	14.67	15.43
11	0.33	7.81
12	8.33	21.3
13	33.67	32.9
14	113.33	122
15	80.00	73.4
16	38.00	49.4
17	15.00	12.656
18	66.70	64.6
19	3.33	6.03
20	56.67	72.7
21	2.67	3.18
22	3.33	1.77

DEPARTMENT OF SOME SUBJECT OR TECHNOLOGY
CHALMERS UNIVERSITY OF TECHNOLOGY
Gothenburg, Sweden
www.chalmers.se

CHALMERS
UNIVERSITY OF TECHNOLOGY